OPTICAL STUDIES OF GAN-BASED LIGHT EMITTING STRUCTURES

By

JACK BIU LAM

Bachelor of Science in Physics

State University of New York at Stony Brook

Stony Brook, New York

1998

Submitted to the Faculty of the
Graduate College of the
Oklahoma State University
in partial fulfillment of
the requirements for
the Degree of
DOCTOR OF PHILOSOPHY
May 2005

OPTICAL STUDIES OF GAN-BASED LIGHT EMITTING

STRUCTURES

Dissertation Approved:

Jerzy Krasinski

Dissertation Adviser

Xincheng Xie

Nicholas Kotov

David Peakheart

A. Gordon Emslie

Dean of the Graduate College

ACKNOWLEDGEMENTS

I would like to express my sincere appreciation to my thesis advisor Dr. Jerzy Krasinski, for the guidance he has given me, in all areas necessary, in my graduate work and the actual creation of this thesis.

I extend my sincerely gratitude to Dr. Jin-Joo Song for the support and guidance she provided for my research, and for maintaining an excellent research environment in which I greatly benefited.

I would like to thank the members of my thesis committee, Dr. Nicholas Kotov, Dr. Xin-Cheng Xie, and Dr. David Peakheart for proving valuable comments on my work.

I would like to express my deep gratitude to Dr. Paul Westhaus for inviting me to study at Oklahoma State University, and having always found the time to answer all my questions and to address all my needs in any ways possible.

I would like to thank my reseach colleagues and friends Dr. Sergiy Bidnyk and Dr. C. K. Choi for their help in both research and life.

And last, but not least, I would like to thank my family for always having sided by me. I would like to dedicate this thesis to my loving parents.

For my loving parents

Hung Cheung Lam and Mei Ling Ng

TABLE OF CONTENTS

LIST OF TABLES

Table Page

LIST OF FIGURES

CHAPTER I

Introduction

Beginning in the early 1990's, the group-III nitride semiconductors, including InN, GaN, AlN, and their alloys, have received a tremendous amount of attention due to the commercial production of the blue light emitting diode (LED) and the fabrication of blue laser diode (LD), both based on the ternary alloy InGaN, first by Nichia Chemical (Japan) [1]. Since then, Research and development of this material has seen rapid advancement and will find application in many fields, optimistically within next few years.

The most important advantages of the III-nitrides are the wide and direct band gaps, with values of 1.9 eV for InN, 3.4 eV for GaN, and 6.2 eV for AlN. The wide band gaps allow the materials to be used in UV to amber opto-electronic devices. The high bond strength (2.3 eV for GaN [2]) makes the III-nitrides suitable for high temperature while their high breakdown fields (3×10^6 V/cm for GaN [Ref. 2]) allow them to be used in high power devices.

Of the group-III nitrides, GaN is the most extensively studied member. The alloying of GaN with In and Al forming ternary compounds $In_xGa_{1-x}N$ and $Al_xGa_{1-x}N$ allows the band gap to be continuously tuned from 1.9 eV to 6.2 eV. Moderate ($x < 0.2$) Al and In molar concentration of alloying are more mature, and found a myriad of applications in the near-UV to green spectral range. GaN crystallizes in cubic (zincblende), rock salt, or hexagonal (wurtzite) structure, with the last being by far most common. The conduction band minimum of wurtzite GaN has Γ_7-symmetry with a quantum number of $J_z = 1/2$. The maximum of the valence band is also located at the Γ-point, resulting in a direct fundamental band-gap. The valence band in GaN is split into three different sub-bands, denoted by *A*, *B*, and *C* by crystal-field and spin-orbit coupling. The *A*-band has Γ_9-symmetry, while *B* and *C* have Γ_7-symmetry. The structure and symmetries of the bands are shown in Figure 1.1 [3].

Table 1.1 contains the relevant basic material parameters of GaN, AlN, and InN. These three materials cover the wavelength range from red to deep UV. A major issue associated with nitride material is lattice matching when growing such thin films on substrates. Besides expensive GaN substrates, only are practical substrates and are widely used. Still large lattice mismatch occurs even with sapphire and SiC, resulting in large strain exist in the grown structures and detrimentally large number of dislocations. Recently free standing GaN thick layers are being used as substrates, producing good results [9]. Figures 1.2 and 1.3 show photoluminescence (PL) and absorption spectra of two different GaN epilayers, respectively. Excitonic resonance associated with the A, B, and C valence band can be seen in the 10 K absorption curve of the 0.38 μm GaN epilayer. PL spectra show free exciton emission dominates over bound exciton emission as temperature increases.

GaN was being synthesized as early as 1938, by Juza and Hahn [4]. Small needles of GaN were synthesized by passing ammonia over hot gallium. In 1969, the first large area GaN layers was deposited by Maruska and Tietjen using the chemical vapor deposition method [5]. The development of p-type doping by Akasaki and Amano in 1989 [6] and the development of suitable epitaxial growth techniques such as metalorganic chemical vapor deposition (MOCVD) made possible p-n junction devices with III nitrides. During the last decade, a number of III-nitride base opto-electric products have been commercialized, including blue, green, and white LEDs, as well as blue and UV LDs. Still immense effort around the world, in industries as well as in universities, are involved in perfecting these devices and bringing out new products, such as the III nitride based UV photodetectors and quantum cascade lasers. This thesis will

deal with the optical emission properties and mechanisms of the GaNs and their In, Al alloys in different temperature and optical excitation conditions.

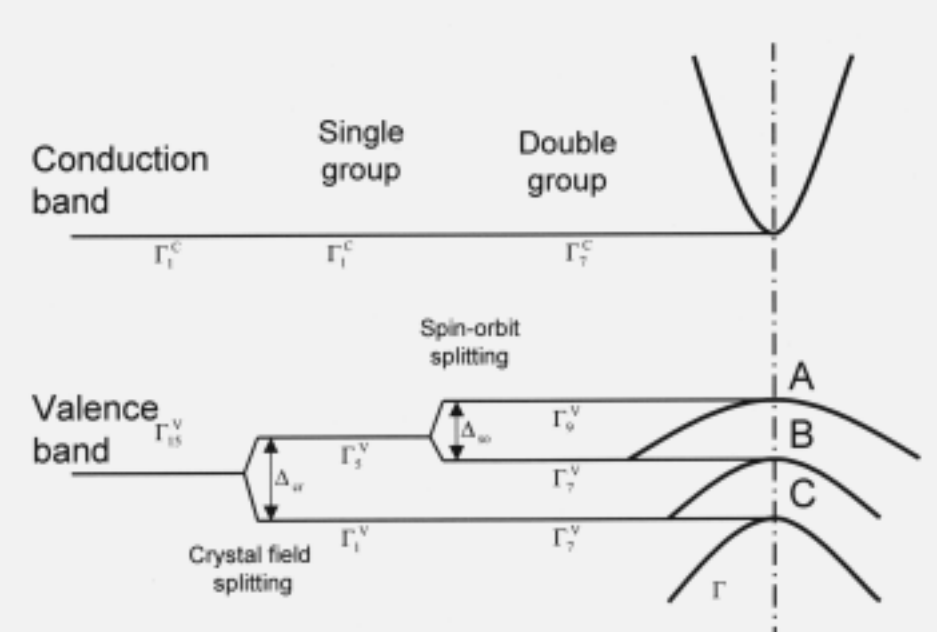

Figure 1.1. Structure and symmetries of the lowest conduction band the uppermost valence bands in wurtzite GaN at the Γ−point.

	GaN	AlN	InN
Band-gap E_g	3.39 eV (300 K) 3.50 eV (1.6 K)	6.2 eV (300 K) 6.28 eV (5 K)	1.89 eV (300 K)
Lattice constants a c	3.189 Å 5.185 Å	3.112 Å 4.982 Å	3.548 Å
Thermal expansion $\Delta a/a$ $\Delta c/c$	5.59×10^{-6} K^{-1} 3.17×10^{-6} K^{-1}	4.2×10^{-6} K^{-1} 5.3×10^{-6} K^{-1}	
Thermal conductivity k	1.3 W/cm K	2 W/cm K	
Index of refraction n	2.33 (1 eV) 2.67 (3.38 eV)	2.15 (3 eV)	2.80 - 3.05

Table 1.1. Basic parameters of GaN, AiN, and InN [7,8].

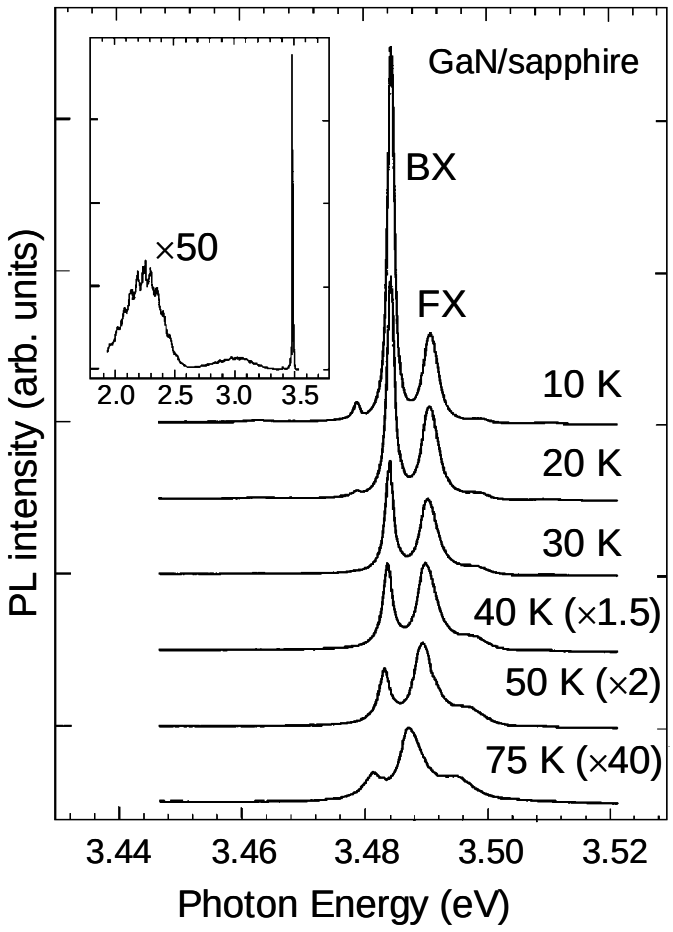

Figure 1.2. Photoluminescence spectra as a function of temperature of a 7.2-μm-thick GaN epilayer. The inset shows the spectrum of the sample over a wider range of photon energies taken at 10 K [10].

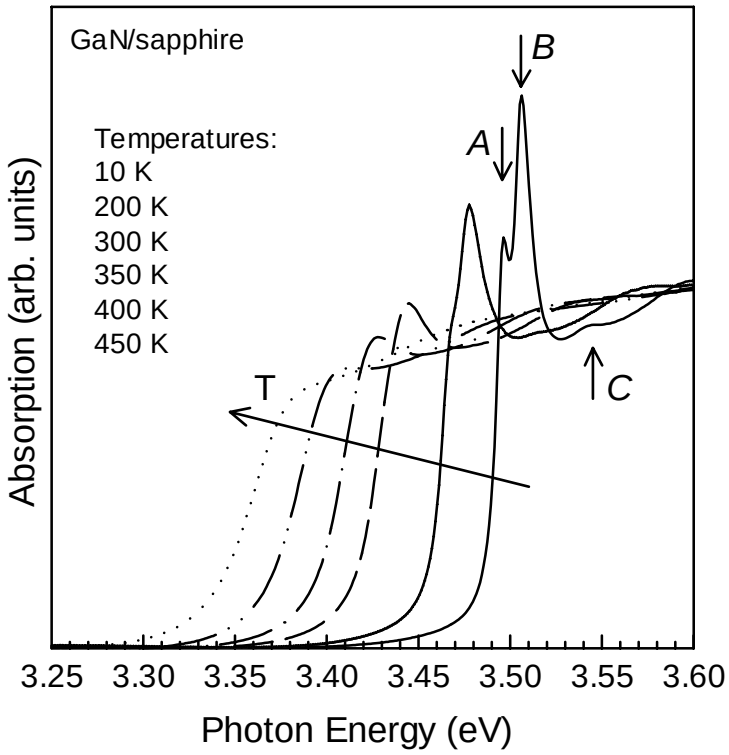

Figure1.3. Absorption spectra of a 0.38-μm-thick GaN. At 10 K, excitonic features associated with the *A*-, *B*-, and *C*- excitons are observed [10].

CHAPTER II

Stimulated Emission and Gain Mechanism in AlGaN

Due to their wide bandgaps, GaN and its Al and In alloys have recently attracted considerable scientific interest for their ultraviolet (UV)-blue-green photonic device applications [11]. In particular, the alloy $Al_xGa_{1-x}N$ is a promising material for light emitting devices and detectors covering almost the entire deep UV spectral range (3.39 - 6.20 eV at room temperature depending on x) with applications including secure from ground interception satellite-to-satellite communication, chemical and flame sensing, and compact tunable UV laser sources for medical purposes. AlGaN-based structures have been shown to possess superior waveguiding properties[12] resulting in lowering of threshold and efficient lasing in GaN/AlGaN heterostructures [13]. The variable stripe gain measurements performed by Eckey *et al.*[14] suggested that, under high optical excitation at 1.8 K, phonon-assisted processes play the dominant role in establishing gain in AlGaN epilayers. Recently, Schmidt *et al.*[15] reported the observation of stimulated emission (SE) in AlGaN epilayers with Al concentrations as high as 26% with SE wavelengths as short as 328 nm. Even though SE mechanisms in GaN epilayers [16] and GaN/AlGaN separate confinement heterostuctures [13] have been thoroughly explored, more studies on the temperature-dependent characteristics of SE in AlGaN epilayers are needed to understand their gain mechanism. Here, a comprehensive temperature-dependence study of the optical properties of AlGaN at, below, and above the SE threshold from 30 to 300 K is presented. The SE threshold and the energy positions of the

spontaneous and stimulated emission peaks over the entire temperature range were studied. Absorption and time-resolved photoluminescence (TRPL) experiments were performed. In this study it is established that different mechanisms are responsible for gain in AlGaN and GaN epilayers. Ways to improve SE efficiency in AlGaN samples are also discussed.

The $Al_{0.17}Ga_{0.83}N$ layer used in this study was grown by low-pressure metalorganic chemical vapor deposition on (0001) sapphire at a temperature of 1050°C. There is a thin (~50 Å) AlN buffer layer between the sapphire and the AlGaN layer, deposited at a temperature of 625°C. Triethylgallium, triethylaluminum, and ammonia were used as precursors in the growth of the $Al_{0.17}Ga_{0.83}N$ layer, which had a thickness of 2.5 μm. The high-density part of this study was performed in the traditional edge emission geometry using a tunable dye laser pumped by a frequency-doubled, injection-seeded Nd:YAG laser. A nonlinear crystal was used to double the frequency into the UV wavelength region. The resulting excitation pulse had a wavelength of 315 nm and had a pulse width of 4 ns. Spontaneous emission experiments were performed in the surface emission geometry to avoid re-absorption effects [17], using a frequency-doubled Ar^+ cw laser (244 nm) as the excitation source. Absorption measurements were performed in the transmission geometry on pieces of the sample etched to a thickness of 0.4 μm using a high energy plasma etching technique. Carrier lifetimes were measured by time-resolved photoluminescence experiment using a picosecond pulsed laser system consisting of a cavity-dumped dye laser synchronously pumped by a frequency-doubled modelocked Nd:YAG laser for excitation and a streak camera for detection. The output pulses from the dye laser had a pulse width of less than 5 ps and a nonlinear crystal was used to

frequency doubled the laser pulse into the UV spectral region. The overall time resolution of the system was better than 15 ps.

Emission spectra of the $Al_{0.17}Ga_{0.83}N$ sample as a function of excitation pump density near the SE threshold are shown in Figs. 2.1 (a) and (b) for 30 K and 300 K, respectively. At low excitation densities, only a broad spontaneous emission peak is seen at ~3.70 eV (~3.59 eV), which had a full width half maximum (FWHM) of 38 meV (150 meV) at 30 K (300 K). As the excitation pump density increases to values exceeding the SE threshold a spectrally narrower peak with a FWHM of 24 meV appears on the low energy shoulder (~3.64 eV) of the spontaneous emission, as shown in Fig. 2.1(a). We note that the intensity of the SE increases superlinearly with excitation power and appears to be strongly transverse-electric (TE) -polarized. A similar behavior was observed at room temperature, as shown in Fig. 2.1(b). When the temperature was raised from 30 to 300 K, the SE threshold increased from 0.3 MW/cm^2 to 1.1 MW/cm^2.

Absorption measurements were performed on pieces of the sample that were etched to 0.4 μm. Thinned AlGaN epilayers are necessary to obtain a high signal-to-noise ratio due to the high optical thickness of AlGaN. The absorption edge appears to be blueshifted by 217 meV (215 meV) at 30 K (300 K) in comparison to the absorption edge of GaN epilayers [18]. The spectral width of the absorption edge of the sample (see Fig. 2.1) is very narrow (~40 meV) at 30 K, which suggests that potential fluctuations associated with aluminum incorporation are much smaller in AlGaN alloys than In composition fluctuation in InGaN alloys [19] (for approximately the same molar fraction). From the absorption data we evaluated the penetration depth of the pump beam

to be $d = 1/\alpha = 1 /(9 \times 10^4 \text{ cm}^{-1}) = 0.11$ μm, where α is the absorption coefficient of the AlGaN sample.

In order to understand the origin of SE in the AlGaN epilayer, we measured the positions of the spontaneous and stimulated emission peaks in the $Al_{0.17}Ga_{0.83}N$ sample at temperatures ranging from 30 to 300 K (see Fig. 2.2). Interestingly, the spontaneous emission peak is seen to blueshifts with increasing temperature up to 75 K and redshifts thereafter. This type of anomalous temperature behavior is qualitatively different from that observed in GaN epilayers and cannot be adequately described by the Varshni equation [20]. There are two plausible explanations for this anomalous temperature behavior of the photoluminescence (PL) peak in AlGaN epilayers. Both piezoelectric fields [21] and potential fluctuations due to composition inhomogeneity [22] have been found to substantially affect the energy position of the main emission peak in InGaN structures, sometimes causing similar kind of anomalous behavior.

By comparing the energy difference between the spontaneous and stimulated emission peaks for the $Al_{0.17}Ga_{0.83}N$ sample over a wide temperature range (see the inset of Fig. 2.2), one can extract additional information as to the origin of gain in AlGaN alloys. Note that for high-quality GaN epilayers, at low temperature, the energy difference between the spontaneous and stimulated emission peaks approaches a constant exciton binding energy [23] and the gain was determined to be due to exciton-exciton scattering [16]. The SE peaks for the AlGaN sample used in this study is located at substantially lower energies than the spontaneous emission peaks. These energy differences increase from about 70 meV at 30 K to over 100 meV at room temperature. Since the exciton binding energy in this sample is expected to be in the range of 20 to 30

meV [18], one can conclude the nonparticipation of excitons in SE. Such a large energy difference between the two peaks is a consequence of band-gap renormalization effects associated with a high carrier density necessary to reach threshold, and thus it is very likely that SE is due to electron-hole plasma (EHP) recombination.

To further corroborate the point that excitons do not take part in establishing gain in the AlGaN sample studied, the behavior of the SE threshold and carrier lifetime with temperature are carefully study, as shown in Fig. 2.3. Note that the carrier lifetime in AlGaN at low temperature is much longer (250 ps) than that observed in GaN epilayers (35 ps) [24]. The difference in carrier lifetime can be explained by either the presence of a piezoelectric field or potential fluctuations due to compositional inhomogeneity. However, the increase of carrier lifetime was not concurrent with a dramatic lowering of the SE threshold, contrary to the case of InGaN. At room temperature, the SE threshold of AlGaN is about 1.8 times that of a high quality GaN epilayer [16]. The SE threshold monotonously increases with increasing temperature. The SE threshold carrier density at 30 K can be readily evaluated if we take into account the recombination lifetime (250 ps) and penetration depth (d = 0.11 μm) of the sample, and a pump density of 0.37 MW/cm^2 (the threshold value at 30 K) roughly corresponds to a carrier density of 1.3×10^{19} cm^{-3}. This value is one order of magnitude larger than the expected value for the Mott density of 1.1×10^{18} cm^{-3} in GaN samples [13], at which point electron-hole interaction is screened by free carriers generated by optical excitation. Excitons are likely to be screened out at these high carrier densities in AlGaN as well, leaving an electron-hole plasma as the only plausible gain mechanism. At elevated temperatures, reaching the SE threshold in AlGaN requires even higher levels of optical excitation. It should be noted

that, as in the GaN SE mechanism study, lifetime measurements were done at relatively low excitation levels, generating carrier densities of only about 5×10^{16} cm^{-3}. Carrier lifetime at near threshold density could be lower. Thus the above estimate of threshold carrier density is only an upper limit.

The results of this study show that AlGaN is a viable material for UV LED and LD applications. We observed a longer carrier lifetimes in the AlGaN sample compared to GaN epilayers. We note that, contrary to what was observed in InGaN alloys [25,26]1 the increase in carrier lifetime did not result in a large reduction in the SE threshold in AlGaN structures. Further improvements in sample quality are needed to reduce non-radiative recombination channels and increase SE efficiency. Also note that the observation of excitons in AlGaN is likely to be related to the crystalline quality of this material. Figure 2.4 shows absorption spectra of the sample at different temperatures. At the lowest temperature of 30 K, there is a slight indication of excitonic feature and that goes away at higher temperatures. As better quality A1GaN sample are grown, it might be possible to observe the effects of excitons on recombination dynamics in A1GaN even at carriers densities close to the SE threshold.

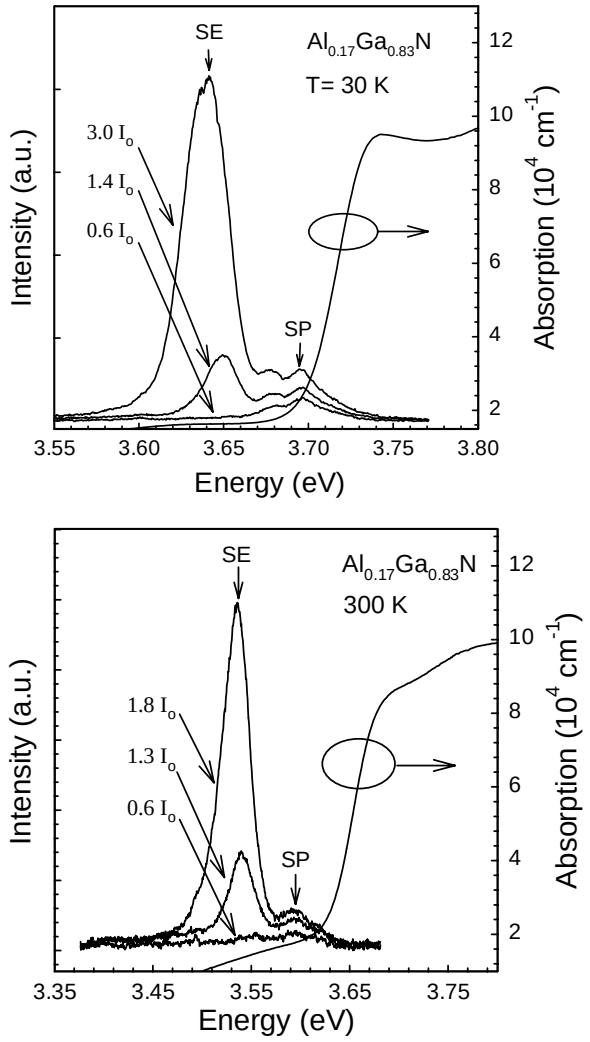

Fig. 2.1. Stimulated emission spectra for the $Al_{0.17}Ga_{0.83}N$ sample at (a) 30 K and (b) room temperature as a function of excitation pump density. SE and SP label the stimulated and spontaneous emission peaks, respectively. The absorption spectra of the sample for both temperatures are also shown.

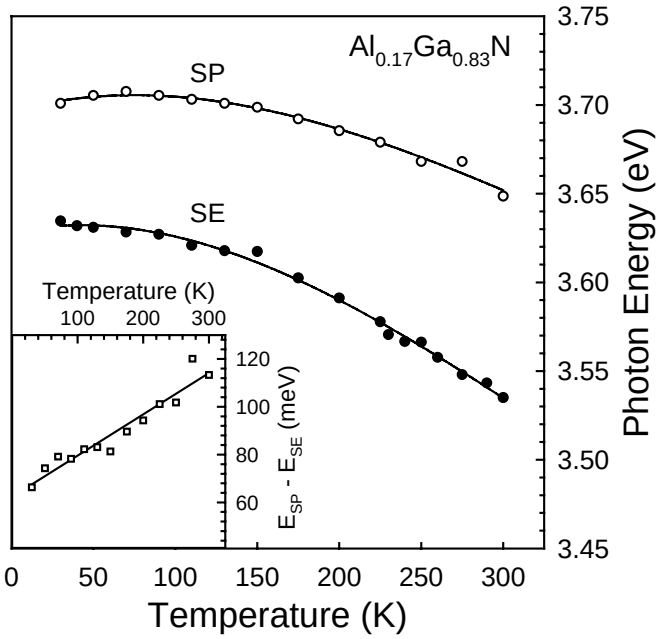

Fig. 2.2. Photoluminescence and stimulated emission peak position as functions of temperature for the $Al_{0.17}Ga_{0.83}N$ sample. The inset shows the energy difference between positions of the PL (open circles) and SE (close circles) peaks versus temperature. The solid lines are to guide the eye only.

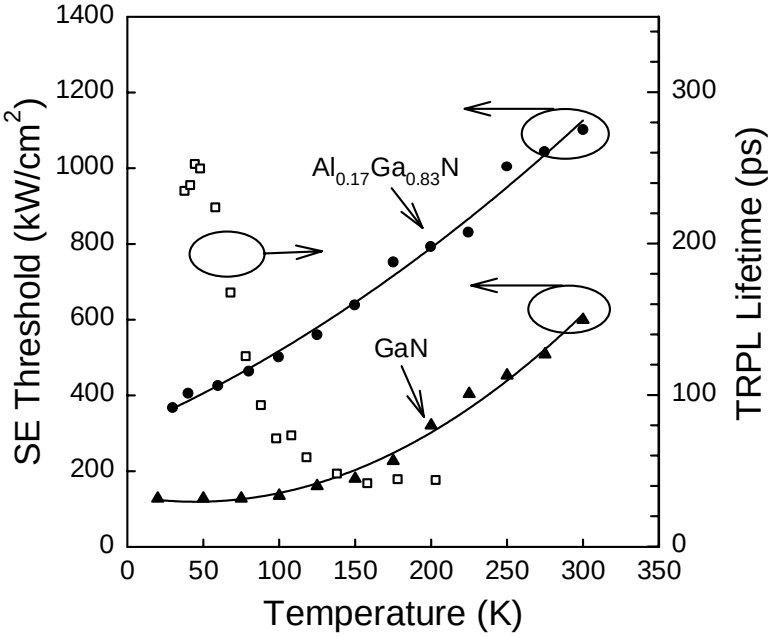

Fig. 2.3. Stimulated emission threshold vs temperature for the $Al_{0.17}Ga_{0.83}N$ sample (closed circles). SE threshold of a GaN epilayer (close triangles) are shown in the figure for the purpose of comparison. Carrier lifetimes (open squares) of the $Al_{0.17}Ga_{0.83}N$ sample as measured by TRPL are also shown as a function of temperature. The solid lines are to guide the eye only.

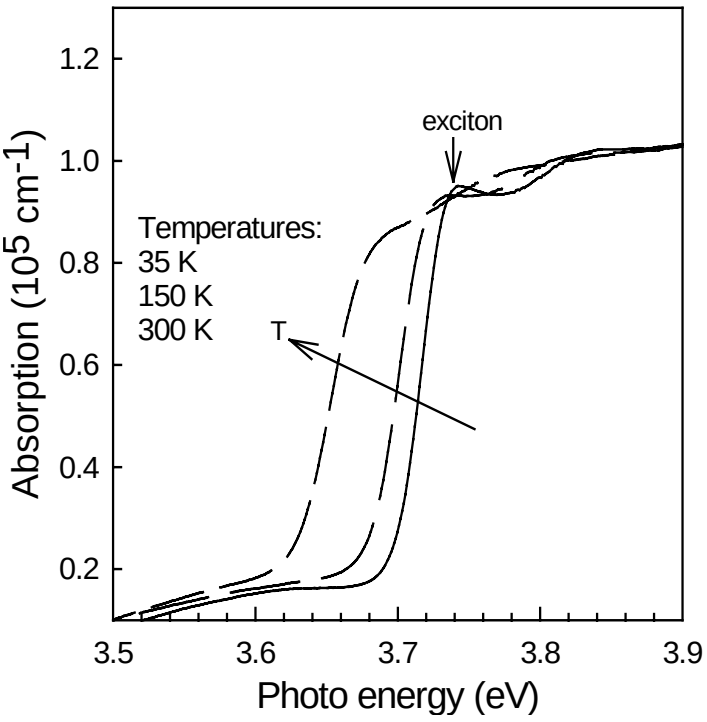

Figure 2.4. Absorption spectra of the AlGaN sample.

CHAPTER III

HVPE-Grown GaN Strutures

With the commercial availability of InGaN-based laser diodes (LDs) and light emitting diodes (LEDs) [27], GaN related materials have proven themselves to be extremely instrumental for the development of optoelectronic devices that operate in the blue-green to UV spectral range. For example, optically pumped lasing at room temperature was obtained in a GaN/AlGaN structure at 362 nm [28], which is shorter than the lowest emission wavelength of 376 nm reported for InGaN-based LDs [29]. Currently, most nitride LEDs and LDs are grown by MOCVD. However, hydride vapor phase epitaxy (HVPE) has become an important growth technique for GaN, since it is a cost-effective way of growing thick, high quality GaN with growth rates of up to 100 μm/h [30] and dislocation densities on the order of 10^6 cm^{-2} [31]. Free-standing HVPE-grown GaN films with thicknesses of up to 300 μm have been produced via laser liftoff [32], and the thicker one grows the GaN layer, the less dislocation it has. Free standing thick GaN films can be used as substrate to grow active nitride structures, avoiding the problem of lattice mismatching when using other material as substrate. Nichia and NEC both have fabricated InGaN-based LDs on HVPE-grown GaN substrates [33,34]. However there are very little studies on the potential of using the HVPE grown nitride structure as the actual light emitting devices. Here, we compare the optical properties of HVPE-grown samples (a GaN epilayer and a GaN/AlGaN double heterostructure) with a high quality MOCVD-grown GaN epilayer, in gain insight into the potentials of HVPE-grown structures.

The HVPE-grown GaN epilayer and the GaN/AlGaN double heterostructure (DH) used in this study were grown using ammonia, GaCl, and $AlCl_3$ as the N, Ga, and Al sources, respectively. The GaN epilayer is 5 μm thick and was deposited on a 5 nm thick AlN buffer layer on a sapphire substrate. The GaN/AlGaN DH was grown on a SiC substrate and has a ~ 250 nm active GaN layer embedded between an $Al_{0.06}Ga_{0.94}N$ layer on top and an $Al_{0.16}Ga_{0.84}N$ layer below. Both AlGaN layers are 400 nm thick. This DH was designed for better optical confinement, and the top AlGaN layer has a smaller Al concentration than the lower AlGaN layer in order to facilitate p-doping the top layer, in case we later choose to do this for making electrical contacts. The MOCVD GaN epilayer is 7.2 μm thick and was grown on a ~ 5 nm AlN buffer layer on a sapphire substrate.

Photoluminescence (PL) experiments were performed using the 244 nm line of an intracavity doubled cw Ar^+ laser. Time-resolved PL (TRPL) measurements were performed using a streak camera for detection. The sample was optically excited by a picosecond pulsed laser system consisting of the second harmonic of a cavity-dumped dye laser synchronously pumped by a frequency-doubled modelocked Nd:YAG laser. The TRPL system has an overall temporal resolution of better than 15 ps. The high-carrier density part of this study was performed in the traditional edge emission geometry using the third harmonics of an injection-seeded Nd:YAG laser and the second harmonic of a tunable dye laser pumped by a frequency-doubled, injection-seeded Nd:YAG laser. A closed-cycle helium cryostat was used to vary the temperature of the samples.

PL spectra from the 5 μm HVPE-grown GaN at 10 K and room temperature (RT) are shown in Figure 3.1. At 10 K, bound exciton emission is observed at 3.474 eV (356.9 nm) with a FWHM of 4.9 meV, and the free A exciton peak is seen as a shoulder

about 6 meV higher in energy. Room temperature PL shows free exciton position at 3.417 meV (362.8 nm) with a 32 meV FWHM. These PL peaks are red shifted by 10 meV (14 meV) from those of the MOCVD-grown GaN at 10 K (RT). The shift may be due to a decrease in the energy bandgap of the HVPE-grown GaN epilayer caused by a reduction in the lattice mismatch induced compressive strain [35]. The reduction is likely due to a lower grown-in stress at high temperature, which may be a result of the growth conditions [36]. The FWHM of the free exciton peaks of both GaN epilayers are similar at RT, but the MOCVD-grown GaN has a narrower bound exciton FWHM (1.4 meV) at 10 K. Overall the HVPE-grown GaN shows good PL quality, comparable to the high quality GaN piece.

Stimulated emission (SE) was obtained for the HVPE-grown GaN both at 10 K and RT using the third harmonic of an Nd:YAG laser as the excitation source. Figure 3.2 shows RT power dependent emission spectra of the HVPE GaN near the SE threshold. The inset shows integrated intensity as a function of excitation density. A sharp transition from spontaneous to stimulated emission was observed to occur at the SE threshold. In addition, the SE is highly polarized, with a TE:TM ratio of 50. The RT SE threshold for this epilayer was measured to be 710 kW/cm^2, which is similar to that of the MOCVD-grown GaN (600 kW/cm^2). At 10 K, the SE threshold of the HVPE GaN is 200 kW/cm^2, which is lower than the 300 kW/cm^2 threshold of the MOCVD GaN. The RT SE peak of the HVPE-grown GaN is at 3.310 eV, which is redshifted 107 meV from the spontaneous emission peak. This large shift is due to bandgap renormalization effects, and indicates that electron-hole plasma recombination is the dominant gain mechanism in this epilayer at room temperature, as in the case of the MOCVD GaN [37].

Figure 3.3(a) shows the HVPE-grown GaN TRPL at 10 K with a bound exciton lifetime of 67 ps, which is much longer than the 35 ps lifetime of the MOCVD-grown GaN. The inset shows RT TRPL for the HVPE GaN having a decay time of 48 ps. Figure 3.3(b) shows the temperature dependent integrated PL intensity from 10 to 300 K for the HVPE- and MOCVD- grown GaN epilayers. From 10 to 70 K, the integrated PL intensity of the HVPE-grown GaN decreases faster than that of the MOCVD-grown GaN, as shown in Figure 3(b). However, above 70 K, MOCVD-grown GaN PL intensity decreases more rapidly and has about the same 10 K to RT intensity ratio as the HVPE-grown GaN. This indicates that there is still a large density of non-radiative recombination channels in the HVPE-grown GaN, especially channels activated below 70 K. The exact mechanisms of non-radiative recombination were not studied, but in assuming that the dislocations (and not the point defects) are the dominant non-radiative recombination centers, one would expect an improvement in the quantum efficiency by growing thicker HVPE-grown GaN layers resulting from to a substantial reduction in the density of dislocations farther away from the interface [38].

The HVPE-grown $Al_{0.16}Ga_{0.94}N/GaN/Al_{0.06}Ga_{0.94}N$ DH PL at 10 K and RT, are shown in Figure 4(a). The 10 K PL shows the $Al_{0.06}Ga_{0.94}N$ layer emission peak at 3.586 eV and the GaN emission peaks at 3.459 eV. We obtained 10 K and RT SE in the DH, using the second harmonic of a tunable dye laser at 350 nm (3.542 eV, which is below the band edge of the $Al_{0.06}Ga_{0.94}N$ layer) as the excitation source. This is the first demonstration of SE in a HVPE-grown nitride heterostructure. Figure 4(b) shows RT power dependent emission spectra of the HVPE GaN/AlGaN DH near the SE threshold. The RT SE threshold is measured to be 1.4 MW/cm^2, about twice that of the 5 μm thick

HVPE-grown GaN in Figure 3.2. The increased threshold is attributed to an increased role of non-radiative recombination due to the presence of interfaces. Slightly above the threshold, the RT SE peak is at 3.330 eV, which is redshifted about 100 meV from the PL peak. This again indicates that electron-hole recombination is responsible for the gain in the GaN active layer at room temperature. Figure 3.5 show X-ray measurements and figure 3.6 show a microscopic picture of the HVPE-grown GaN epilayer. While the GaN has a good structural property ,the surface roughness due to rapid growth rate could be a negative factor. To improve the optical quality and reduce the SE threshold, a thicker lower AlGaN layer, a separate confinement heterostructure (SCH) [28], and better interface control should be investigated.

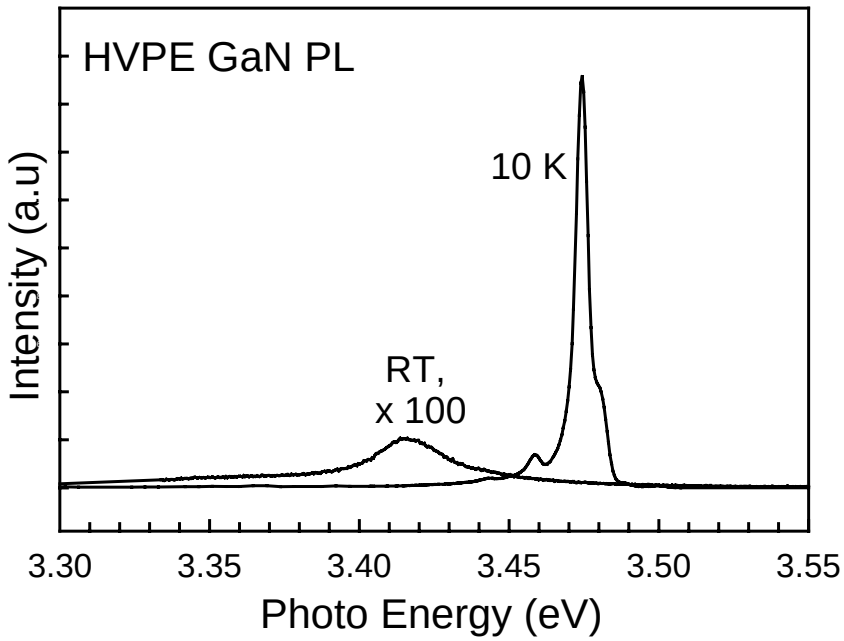

Figure 3.1. 10 K and room temperature photoluminescence for the 5 μm HVPE-grown GaN.

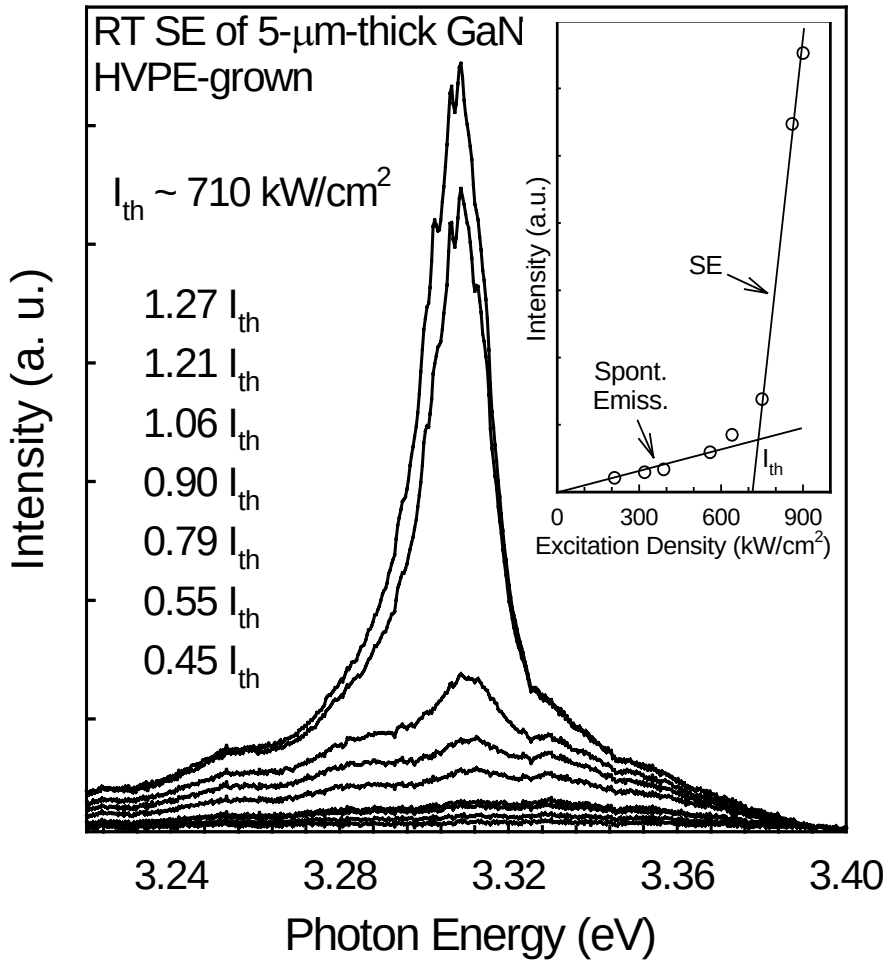

Figure 3.2. Room temperature emission spectra of the 5μm thick HVPE GaN epilayer at various excitation densities near the stimulated emission (SE) threshold (I_{th}). The top curve correspond to the maximum pump power of 1.27 I_{th}, and so on. The inset shows the integrated intensity as a function of excitation density. The lines in the inset are to guide the eye only.

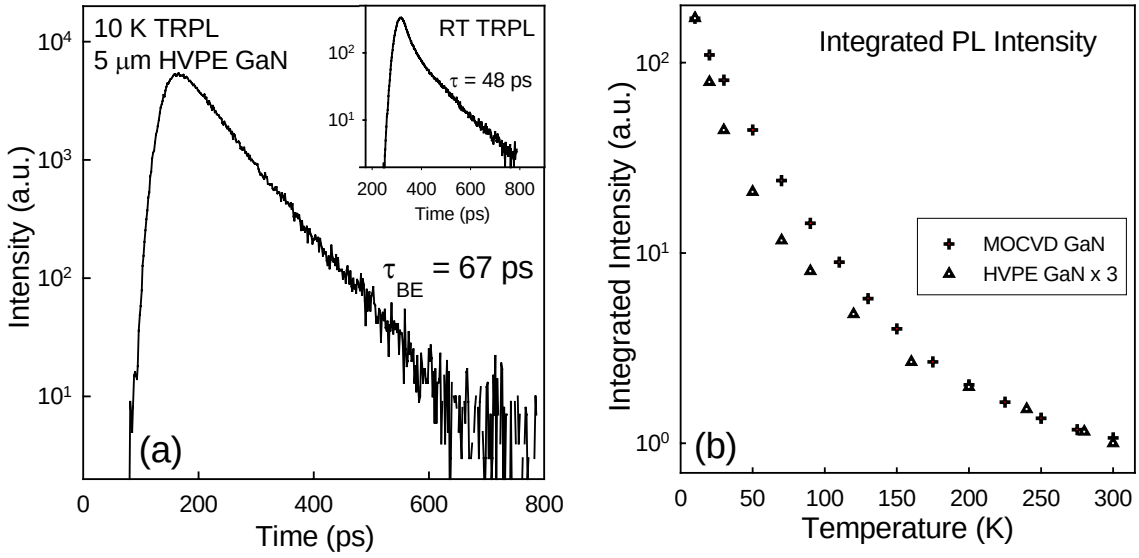

Figure 3.3. (a) Time-resolved photoluminescence of the HVPE GaN epilayer and (b) temperature dependent integrated PL of the HVPE and MOCVD GaN epilayers.

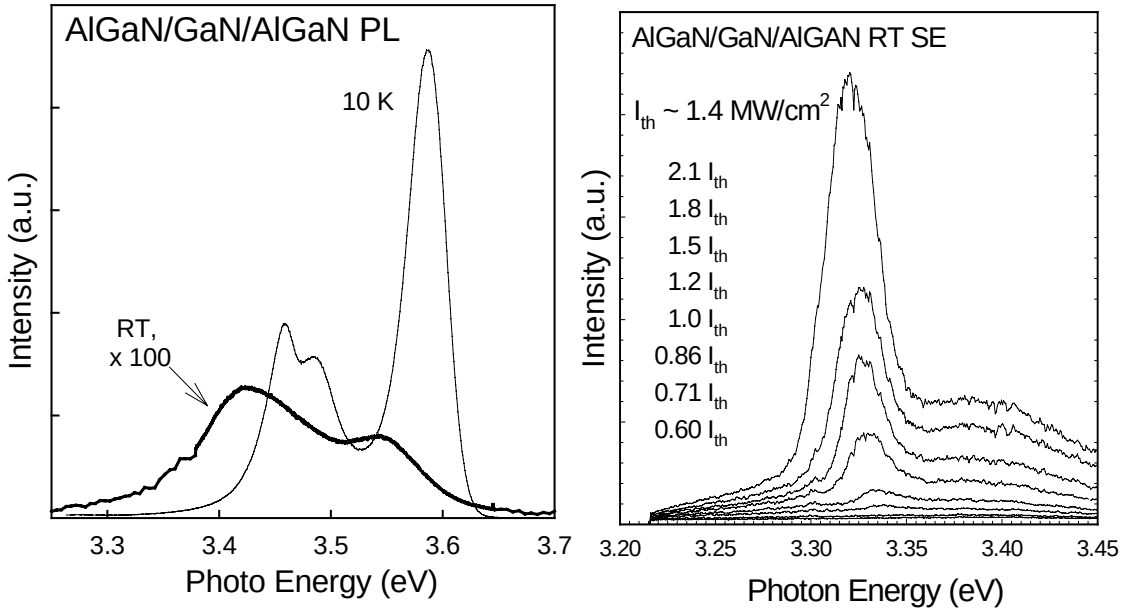

Figure 3.4. (a) Photoluminescence and (b) emission spectra of the HVPE GaN/AlGaN double heterostructure near the stimulated emission (SE) threshold excitation density I_{th}.

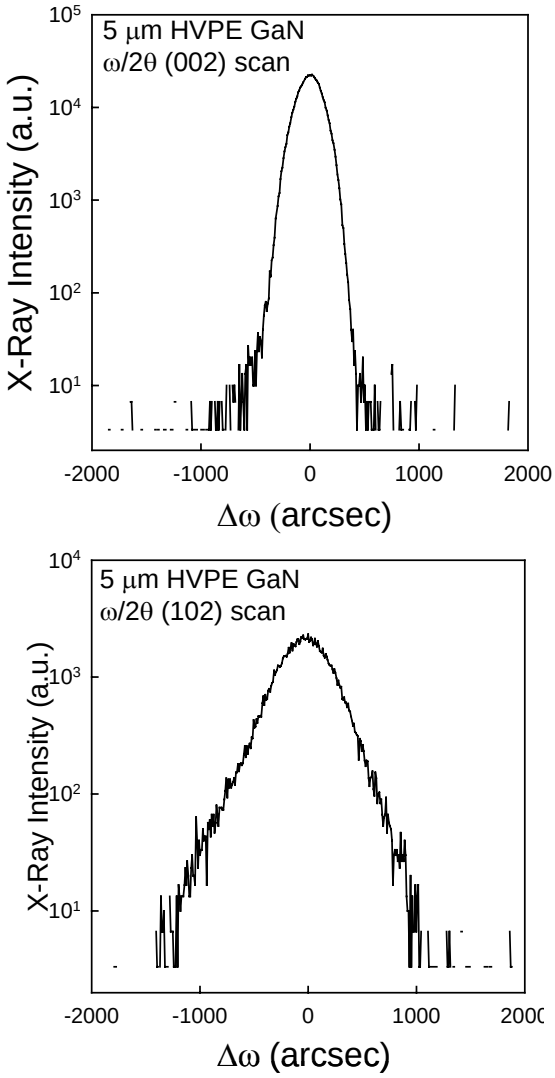

Figure 3.5. X-ray scan of the HVPE-grown GaN. Shows similar FWHM as the MOCVD-grown GaN.

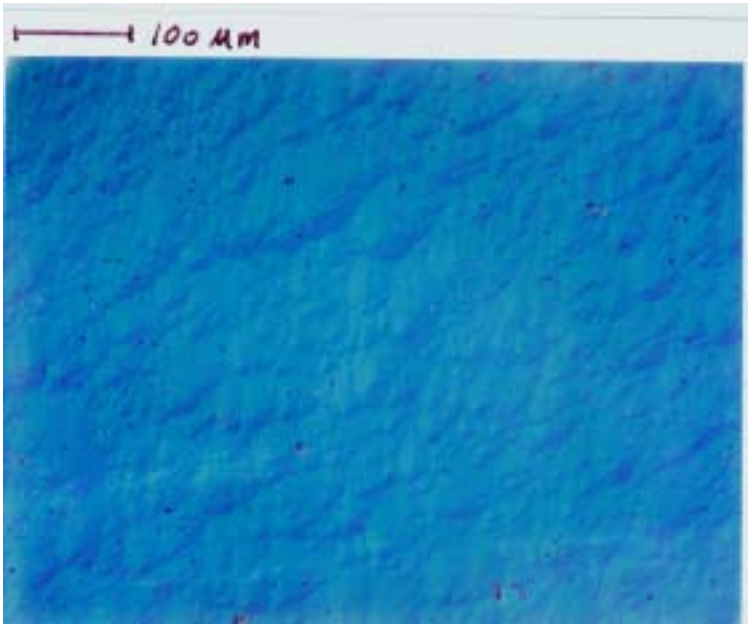

Figure 3.6. Microscopic interferometric (Nomarsky) picture of the surface of the HVPE-grown GaN epilayer.

CHAPTER IV

Optical Emission of InGaN with Low In Content

The alloy InGaN is widely used in GaN based light emitting devices as well layers and/or barrier layers[39,40]. Alloying of In with GaN has a strong effect of increasing the emission efficiency and lowering the lasing threshold and is widely applied in LEDs and laser diodes [41, 42]. Here a study of the effect of incorporation of a very small amount of In into GaN is presented.

In this study the samples were grown on sapphire substrates. They have 1 μm GaN buffer layers, followed by 150 nm thick InGaN active layers, and are capped by 40 nm GaN layers. The In composition in the InGaN active layers are 0.4, 1.5, 2.4 percent for the three samples, achieved through a controlled growth trimethylIn flow rate of 10, 40 and 75 cc/min respectively.

Figure 4.1 shows X-Ray Diffraction measurement of the three samples. Diffraction intensity peaks for InGaN layers can be seen on the left side of the GaN main peaks. The relative positions of the InGaN peaks on the X-ray scan tell the In contents of each sample. The FWHM of the GaN peaks of about 250 arcseconds indicate good crystalline quality for all samples.

Figure 4.2 shows the low temperature (10 K) photoluminescence spectra of the three samples. The main peaks are from the InGaN active layers, from left to right, of the samples containing 0.4, 1.5, and 2.4 % of In. High fluorescence efficiency is observed for all samples at low temperatures. The PL peaks have FWHMs of 9, 28, and 39 meV

respectively. The broadening of the PL spectra is due to increase in composition fluctuation with increasing In content.

Figure 4.3(a) shows the temperature dependents of PL peak energies from 10 K to 300 K. For the 1.5 and 2.4 % In sample, there are clearly S-shape behaviors of peak energy positions as a function of temperature. This indicates the typical carrier localization caused by In fluctuation in the InGaN samples [43]. The S-shape behavior can be explained as follows. For low temperatures, in this case 50 K and below, since the radiative recombination is dominant, the carrier lifetime increases giving them more opportunity to relax down to the localized states, producing a redshift. For intermediate temperatures (50 to 120 K), a rapid increase in nonradiative recombination decreases the carrier lifetime, causing the carriers to recombine before having enough time to travel to the localized states, and results in blueshift of the PL peak position. At higher temperatures (above 120 K) nonradiative processes become dominant and lifetimes are almost constant. Photogenerated carriers are less affected by changes in lifetime, so blueshift behavior become smaller, and the redshift of PL peaks are caused by band-gap shrinkage with increasing temperatures. This effect shows that fluctuation of In composition can occur in InGaN layers with In content as low as one and a half percent. The S-shape behavior becomes more pronounced as In content is increased, showing that composition fluctuation increased as In content increases. In Figure 4.3(b), the integrated PL intensities of the three samples at low temperature and room temperature are shown. The PL intensities drop 3-4 orders of magnitude between 10 K and room temperature. For room temperature, PL intensities increase with higher In incorporation, this indicates increased suppression of non-radiative channels, due to deeper carrier

localization [44,45], and give further evidence that higher In content leads to higher degree of carrier localization.

To further analyze the PL behavior, the integrated PL intensities were plotted as a function of inverse temperature, as shown in figure 4.4. The data are fit with the equation I(T) = a/(1+c1*exp(-E1/kT)+c2*exp(-E2/kT) where I(T) is the temperature dependent intensity, E1 and E2 are activation energies, and a,c1, and c2 are fitting parameters. The activation energy obtained are 6.1, 28 meV for the 1.5% and 7.0, 31 meV for the 2.4% In content samples. This is corroborative to the conclusion that increased in localization depth for samples with higher In contents.

All three samples showed stimulated emission at 10 K and at room temperature. For the 2.4% In, threshold excitation density of 7 kW/cm^2 at 10 K is very low compared to the GaN's threshold of 100 – 300 kW/cm^2, while the SE wavelength is only 8 nm higher. The SE spectra are shown in Fig. 4.5. At 1.5% and 2.4% In composition, the SE threshold dramatically changes between 10 K and RT, as shown in Fig. 4.5(b). The low SE threshold indicates carrier localization effect plays important role in these two samples at 10 K.

In summary, this study shows successful low indium incorporation into GaN. $In_XGa_{1-X}N$ with x values of 0.4, 1.5, and 2.4 % were studied. The S-shaped temperature dependence of PL peak energies indicates indium segregation (typical of InGaN), which causes composition fluctuation and carrier localization leading to higher spontaneous emission intensity at RT. Stimulated emission at both 10 K and room temperature was observed for all three samples. Dramatic decrease of SE threshold is observed as indium content increase to 1.5%.

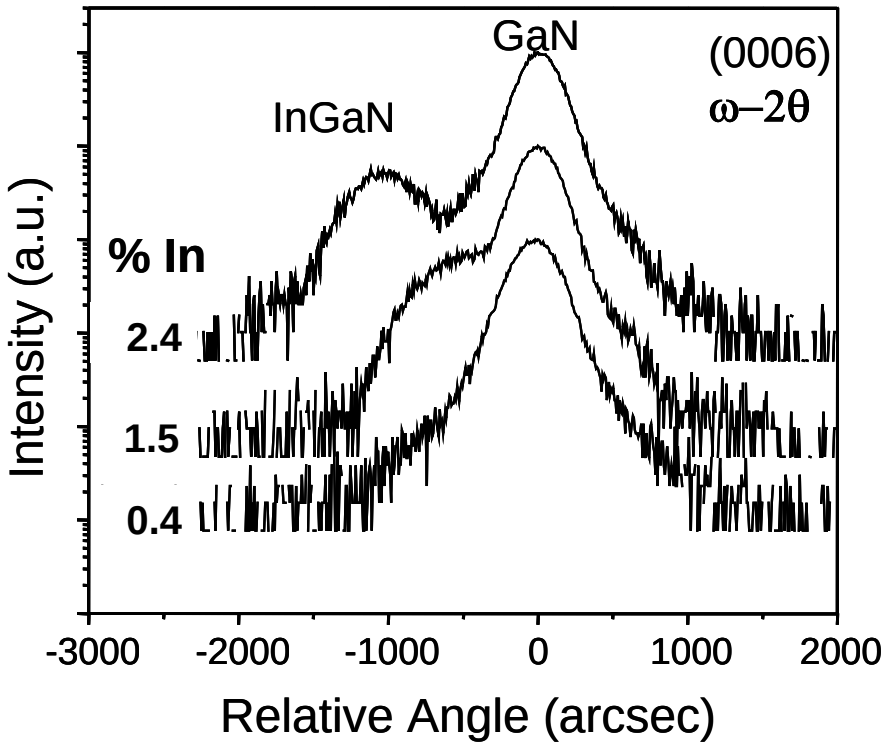

Fig. 4.1. X-Ray diffraction scans of the three InGaN samples.

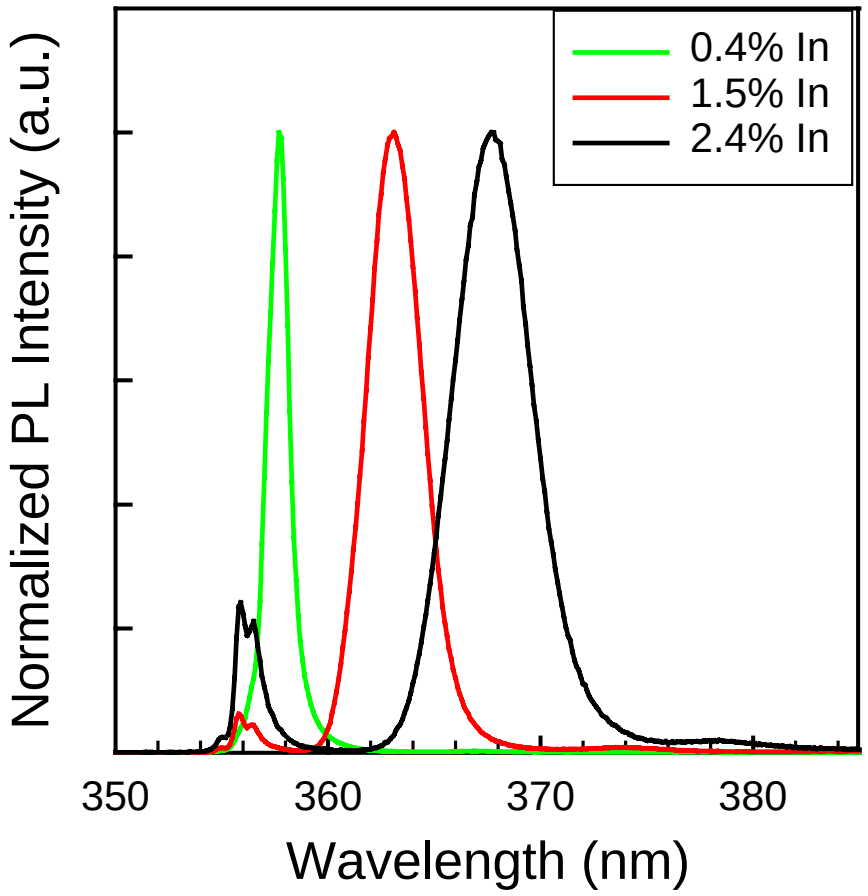

Fig. 4.2. Normalized PL spectra of the InGaN samples. From left to right are the 0.4, 1.5 and 2.4% In sample respectively.

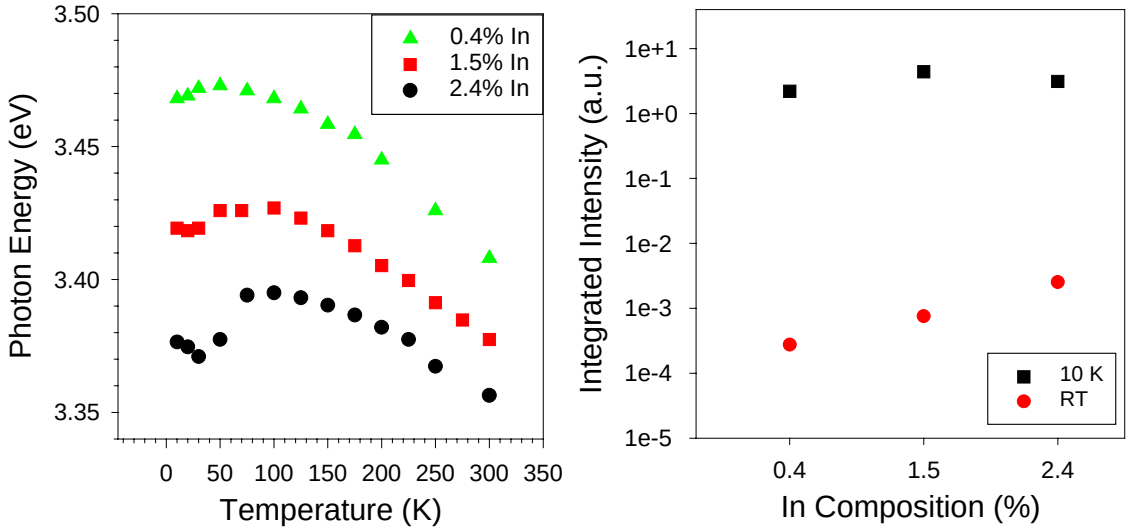

Fig. 4.3. (a)Peak energy position vs. temperature and (b) integrated intensity vs. In content.

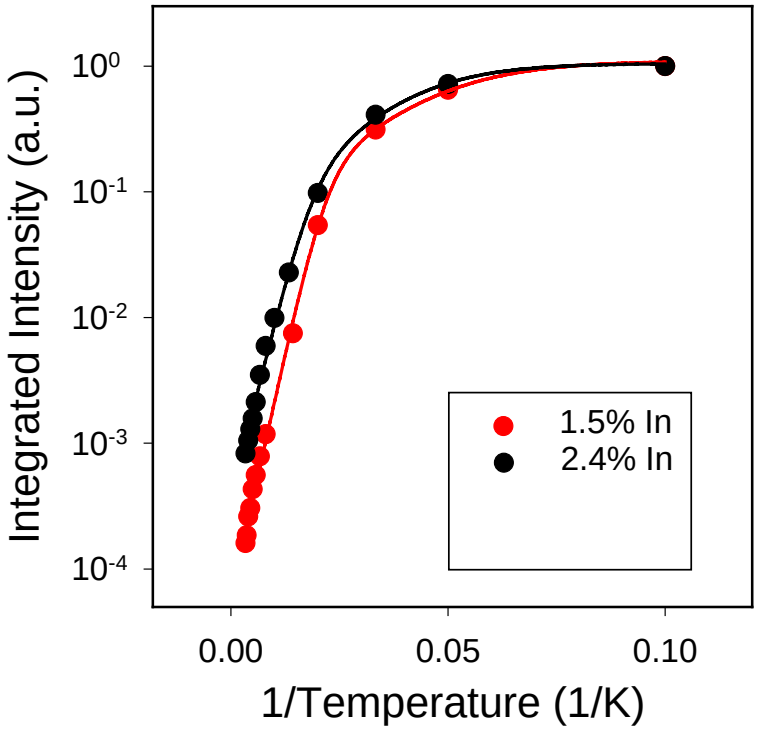

Fig. 4.4. Temperature dependent spectrally integrated intensity of the InGaN samples. The upper curve is of 2.4% In sample, the lower one is of 1.5% In sample. The line shows the fit.

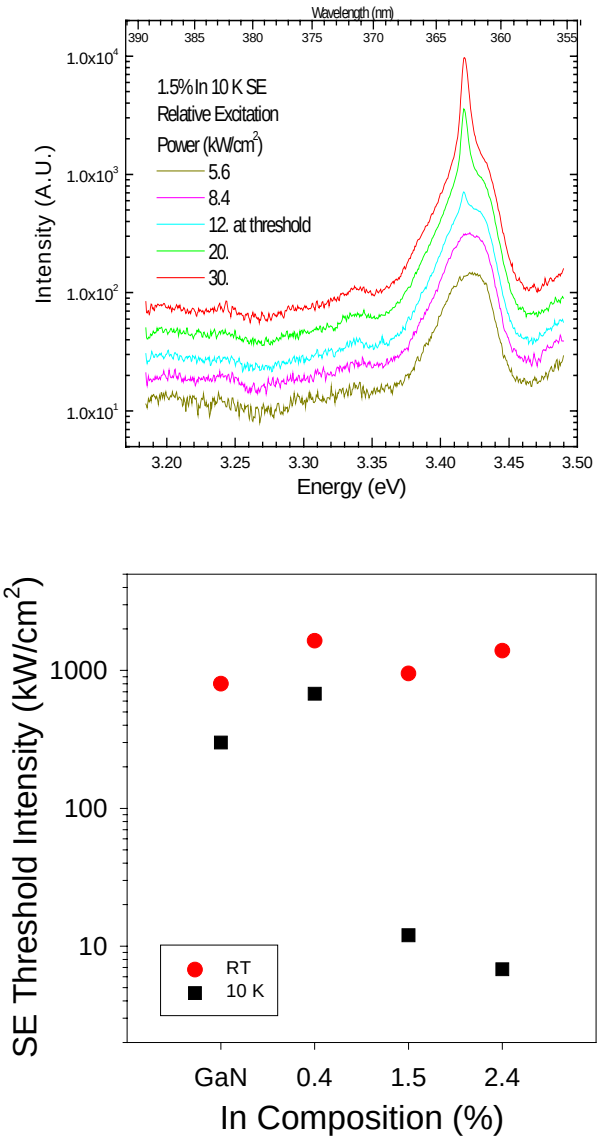

Fig. 4.5. a) Shows the SE spectra of the 1.5% InGaN and b) shows the SE threshold of the samples.

CHAPTER V

Femtosecond Spectroscopy of Highly excited InGaN/GaN Heterostructure

Among the alloys of GaN, $In_xGa_{1-x}N$ proved to be the most efficient in light emitting applications, and is the most used in actual LED and laser diode products, including a long lifetime cw blue diode laser operated at room temperature [46]. Given the large carrier densities required to achieve lasing in these devices, it is necessary to study the carrier dynamics in highly excited $In_xGa_{1-x}N$ thin films. In this chapter the author reports a study on one of such InGaN thin films, using femtosecond nondegenerate pump-probe (PP) spectroscopy as well as TRPL measurements. This study explored the early stage thermalization processes of the hot carriers generated by femtosecond pump pulse, and also the temporal evolution of the recombination process.

The InGaN sample used in the study is a nominally undoped $In_{0.18}Ga_{0.82}N$ layer grown by MOCVD at deposition temperature of 800^o C, with a thickness of 100 nm. It should be noted that the In content could be over estimated. The structure consists of a 1.8 μm GaN buffer layer, follow by a 50 nm silicon doped (~10^{18} cm^{-3}) GaN layer, the $In_{0.18}Ga_{0.82}N$ active layer, and capped by a 50 nm silicon doped (~10^{19} cm^{-3}) GaN layer. Femtosecond PP was carrier out in the surface emission geometry using a pump beam with 355 fs FWHM (measured by difference-frequency mixing in a BBO crystal) at 3.345 eV (295 meV above the absorption edge of excited InGaN sample at 10 K), and a broadband continuum probe beam with a 350 fs pulse width. TRPL measurements were also performed in the surface emission geometry, using a streak camera and a

monochromator. The TRPL system had an overall time resolution of about 60 ps. The excitation energies for PP and TRPL are the same. All measurements were done at 10 K.

Within the sample, since the InGaN conduction band lies at a lower energy state than the GaN:Si donor states, the donor electrons will move into the InGaN region. The self-consistent potential seen by an electron in the sample can be modeled by an effective mass theory taking into account the exchange-correlation potential within the local density approximation. A numerical method [47] is used to calculate the carrier density in the InGaN region due to transfer of donor electrons from the Si doped GaN layer. The resulting 2D carrier densities are 1.1×10^{12} and 7.5×10^{11} cm^{-2} for the interface between the heavily and the less heavily doped GaN layer, respectively. This is not enough to effect the interaction among photo-excited carriers, where carrier densities on 10^{17} cm^{-3} and above are generated.

Figure 5.1 shows the differential transmission spectra (DTS) [48] at early time stages for an average carrier density of 3×10^{18} cm^{-3}, as estimated from band filling [49]. Note that due to absorption within the InGaN region, there is an exponential decay of carrier density in depth, with an absorption coefficient of 1.5×10^{5} cm^{-1} for the InGaN layer. For the rest of the chapter, carrier densities will be meaning the average density in the InGaN region. The inset shows PL spectra (dotted line), the absorption spectra (solid line), and the pump spectra (dash line). The large Stokes shift of ~58 meV between the PL spectra and the absorption edge is due to both band bending near the interface and In composition fluctuations in the alloy [50-53]. The zero time delay is taken to be the maximum of the pump pulse.

Before the time period of –200 fs, no significant changes in transmission of the probe beam were observed. At –200 fs, spectral hole burning [54] is observed to peak at the high energy tail of the pump pulse. At –100 fs, a broad tail at the lower energy side is seen. It arises from the fast interactions between the photogenerated carrier and the electrons that already existed as a result of Si doping. Between 0 and 300 fs, longitudinal optical (LO) phonons can be clearly observed, arising from electron-phonon scattering. At 0 fs time delay, the two broad peaks can be seen to occur at 3.25 eV and 3.18 eV. The spacing is about equally to the expected LO phonon energy of 89 meV, obtained from the linear interpolation on LO phonon energies of 92, and 74 meV for GaN and InN, respectively [55,56]. Note that the observation of successive LO phonon emission does not mean carrier relaxation can be simply explained by LO phonon cascade model. Considering the fact the decrease in density of state with decreasing photon energy will cause the DTS value to increase, the fraction of carriers involved in LO phonon emission is small. Carrier-carrier interaction causing the broadening of nonthermal carrier distribution (giving raise to the broad tail on the lower energy side seen at –200 fs) as well as electron-phonon scattering play a role in relaxation process. The relaxation process is very slow in this material when comparing to the redistribution of hot carriers over a wide energy range within 100 fs [57]. This is due to hot phonon effect where electrons lose energy very inefficiently when LO phonons are as hot as the electrons [58,59].

Figure 5.2 shows the absorption spectra of the InGaN layer as a function of time delay, for average carrier densities of and 4×10^{17} cm^{-3}. For a carrier density of 4×10^{18} cm^{-3}, the average distance between carriers is on the order of 3 nm, which is about the

same as the exciton Bohr radius in GaN. Thus the hot carriers in the InGaN layer form a electron-hole plasma (EHP), where as at a carrier density of 4×10^{17} cm^{-3}, correlations between electrons and holes are possible. As the hot electrons relax toward the bottom of the conduction band, the band gap is renormalized, leading to induced absorption near and below the band edge, as seen in Fig. 5.2 for time delays after 1.3 ps. For carrier density of 4×10^{18} cm^{-3}, as the carriers fill in at the edge of the band, induced absorption turns into optical gain, as seen in Fig 5.2(a), extending across the entire band tail. The gain reaches a maximum value of $\sim 1.2 \times 10^{4}$ cm^{-1}, at 2.5 ps. The oscillation in the gain spectra is due to Fabry-Perot interference. This optical gain at the band edge is similar to that shown by other pump probe spectroscopy studies on bulk GaAs [60], GaAs/AlGaAs multiple quantum wells (MQW's) [61], and InGaN/GaN MQW's [62].

In Fig. 5.2(b), where the carrier density of 4×10^{17} cm^{-3} is not enough to generate optical gain, only induced absorption is seen. At 3 ps, most of the carriers are situated at above the effective mobility edge (E_{em}) [63] (indicated by the arrow) of 3.04 eV, determined by the excitation energy dependence of PL peak positions [64] while there are still states available below. This means that the total density of localized stated resulting from In composition fluctuation is less than 4×10^{17} cm^{-3}. To support this point, in figure 5.4, the PL peak positions do not shift at and below carrier density of 1×10^{17} cm^{-3}, but show significant blue shift at density of 5×10^{17} cm^{-3} due to band filling of localized 1×10^{17} cm^{-3} states. Therefore it can be estimated that the total localized states lies between 1×10^{17} cm^{-3} and 4×10^{17} cm^{-3}.

Figure 5.3 shows the absorption spectra and their corresponding DTS for the sample in the time delay range of 10 to 50 ps, for two carrier densities of 3×10^{18} and 1

$\times 10^{17}$ cm^{-3}. The rate of hot carrier relaxation depends strongly on the number of available lower-energy states. For carrier density of 3×10^{18} cm^{-3}, the recovery of bleaching is much faster than that for 1×10^{17} cm^{-3} carrier density. This point to a very fast carrier depopulation process, i.e. stimulated emission (SE), exist when photoexcited carrier are at such high density. Time resolved PL measurement show that the SE process has a decay time of ~28 ps at carrier density of greater than 1×10^{18} cm^{-3} (see Fig. 5.4). However, comparing to the 1.8 ps time scale for the hot carriers to relax to the absorption edge, as shown in Fig. 5.2, the relaxation processes shown in Fig. 5.3 are very slow. In fact, there is a clamping of carrier relaxation near E_{em} for carrier density of 1×10^{17} cm^{-3}, when there are enough localized states to accommodate for the number of carrier at this density. This is indicative of a mobility edge type behavior in the Mott-Anderson view of localization relating to hot carrier relaxation [65].

Figure 5.4 shows result of TRPL measurements. Fig. 5.4(a) shows the time integrated PL spectra, while (b) shows the time resolved intensities for a number of carrier densities. The threshold carrier density for stimulated emission is found to be 1×10^{18} cm^{-3}, above which the integrated PL intensity show superlinear growth. The rather large threshold density is contributed to the large effective mass [66]. Other study [67] shows that filling of localized states is a prerequisite for lasing in InGaN QW laser diodes. Spontaneous emission is attributed to the recombination of localized carriers since strain induced piezoelectric effect [68] is very small in InGaN layers of such thickness.

At carrier densities below SE threshold, time resolved PL intensity shows single exponential decay and life times in the hundreds of picoseconds. At above SE threshold,

TRPL measurements show two exponential decay, with a fast SE lifetime on the order of ~20's ps.

Figure 5.5 shows the time integrated PL intensity along with effective recombination lifetime (by fitting the decay exponential) at different photon energies across the PL peaks, for three carrier densities. The density of state in the band tail decreases quickly with increasing activation energy, leading to a lower density of final states for acoustic phonon relaxation or tunneling [69,70]. As a result, the average spatial separation between sites with deeper potential increases [71], causing longer effective PL lifetime at lower energies. At energies above E_{em}, decay is likely dominated by the rapid nonradiative migration to lower localized sites and has a much shorter lifetime. This is shown in Fig. 5.5 (a) and (b). In (c), where carrier density is above SE threshold, lifetime is below 30 ps across the peak.

Figure 5.6 shows the temporal evolution of optical emission at two carrier densities. (a) shows evolution of SE spectra for a carrier density of 10^{19} cm^{-3}, and (b) shows evolution of spontaneous emission (SPE)for carrier density of 5×10^{17} cm^{-3}. The first (top one for both carrier densities) is taken at the peak of TRPL decay curves. The evolution of the spectral shapes for SE and SPE are quite different, indicating that the SE does not arise from localized states, as in SPE. The blue shift with increasing time delay in SE is expected for an EHP recombination from renormalized band to band transitions due to depletion of carriers. Together with the fact that the total localized density of state is less than 4×10^{17} cm^{-3}, one can conclude that SE arise from recombination of carriers in the extended states in this sample. Note that in other studies [8], SE from an InGaN MQW is shown to have resulted from recombination of carriers in localized states. In this

InGaN sample, both a small density of localized states (less interface than the MQW resulted in less In composition fluctuation) and high SE threshold (due to small gain length in the experiment geometry) contribute to the fact an EHP recombination being responsible for SE observed in this sample.

In summary, hot carrier dynamics in an InGaN thin film was studied using femtosecond pump probe and time resolved photoluminescence spectroscopy at 10 K. Two successive LO phonon emission was clearly observed. As hot carrier relax, optical gain was observed, resulting in stimulated emission, with a threshold carrier density of 1 $\times 10^{18}$ cm^{-3}. SE was attributed to recombination of an electron hole plasma from band to band transitions.

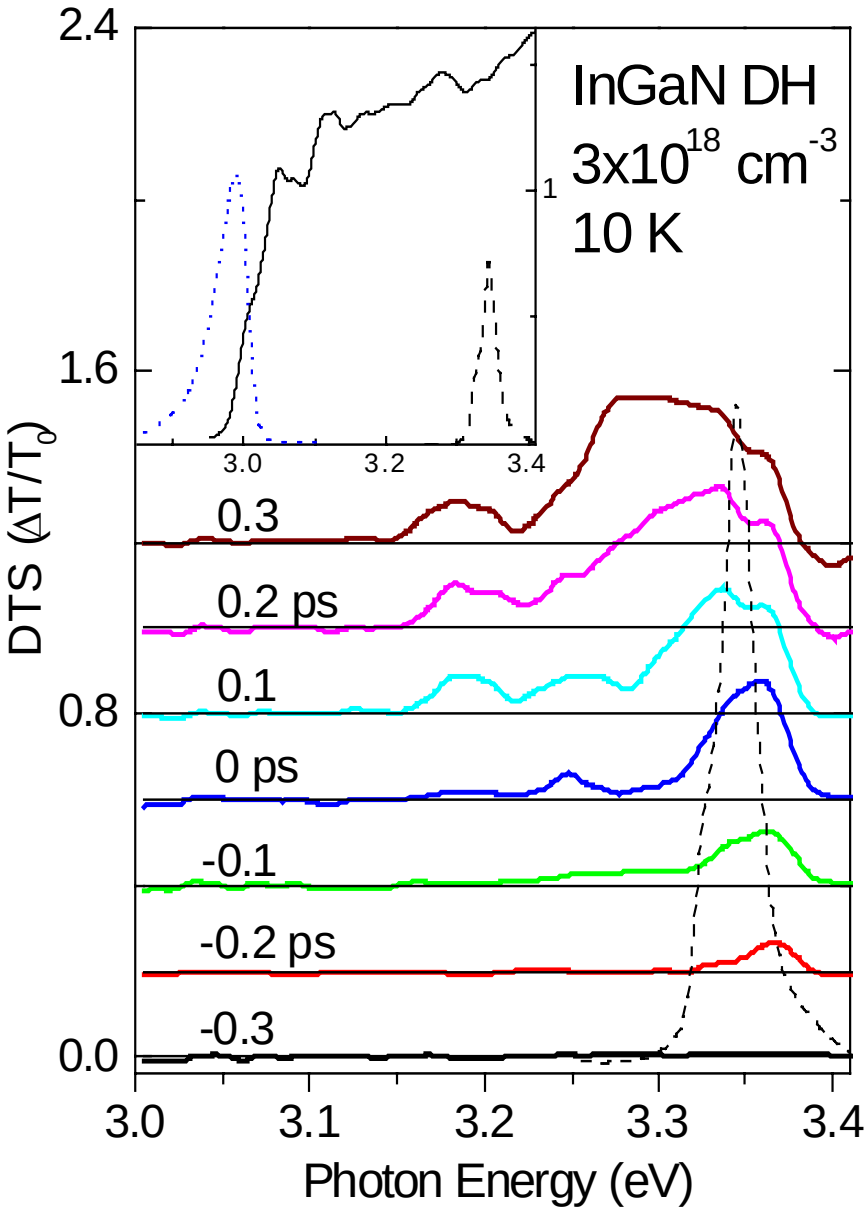

Figure 5.1. Differential transmission spectra (changes in transmission T) of the 100 nm $In_{0.18}Ga_{0.82}N$ active layer at a carrier density of 3×10^{18} cm^{-3}. Inset shows the absorption (solid line), PL (dotted line) and the pump spectra (dashed line).

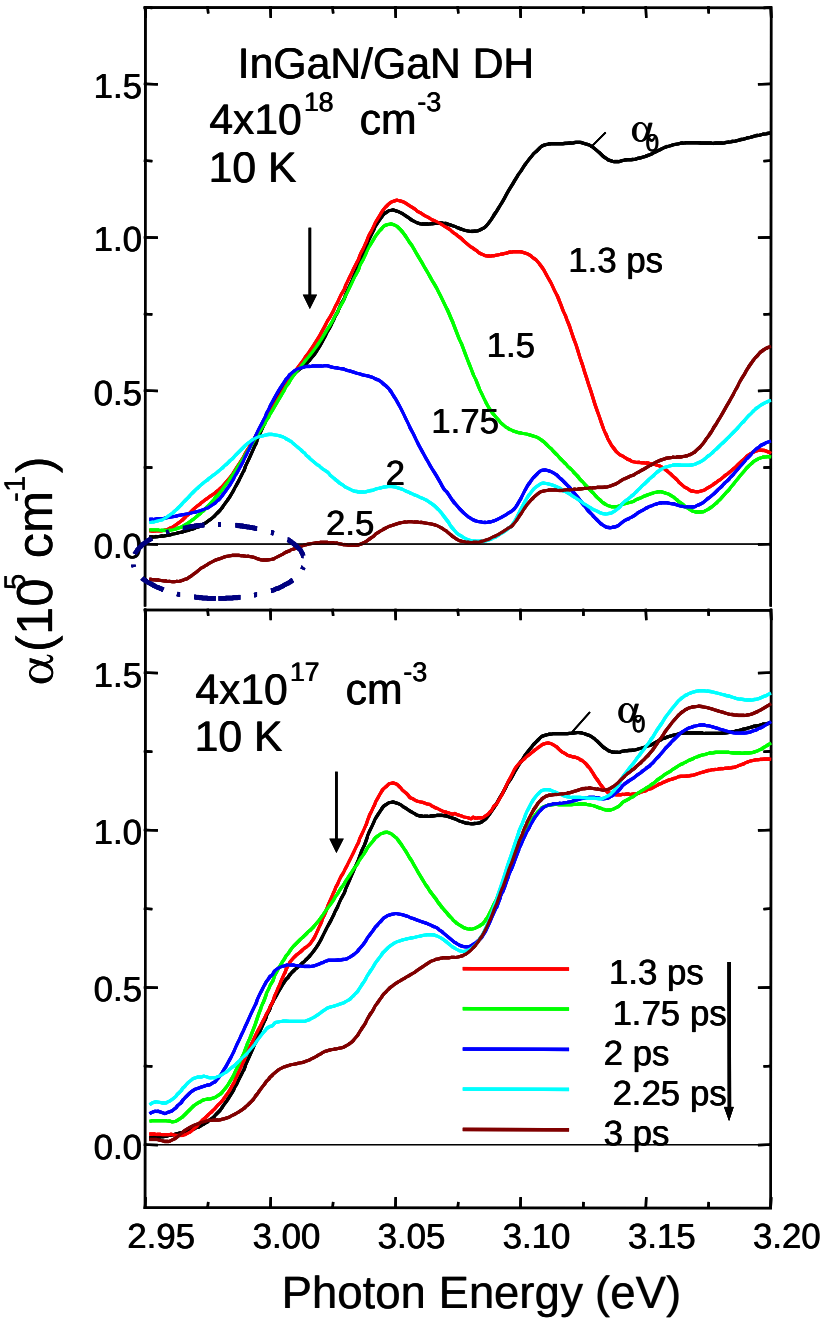

Figure 5.2. Absorption spectra near the band edge as a function of time delay for the InGaN sample for carrier densities of (a) 4×10^{18} cm^{-3} and (b) 4×10^{18} cm^{-3}. The solid line is the absorption without the pump. The arrows indicate effective mobility edge.

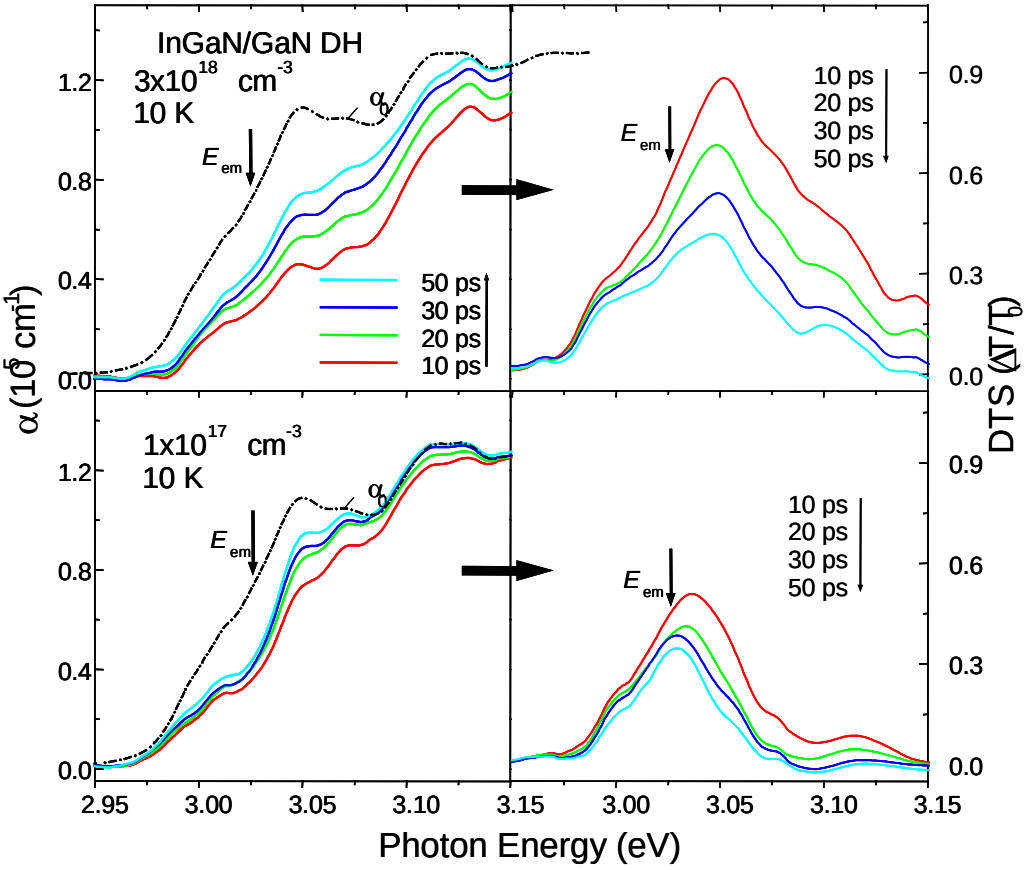

Figure 5.3. Absorption and their corresponding differential transmission spectra of the InGaN sample in the time delay range of 10 to 50 ps, for carrier densities of (a,b) 3×10^{18} cm^{-3} and (b) 1×10^{17} cm^{-3}. The arrows indicate effective mobility edge.

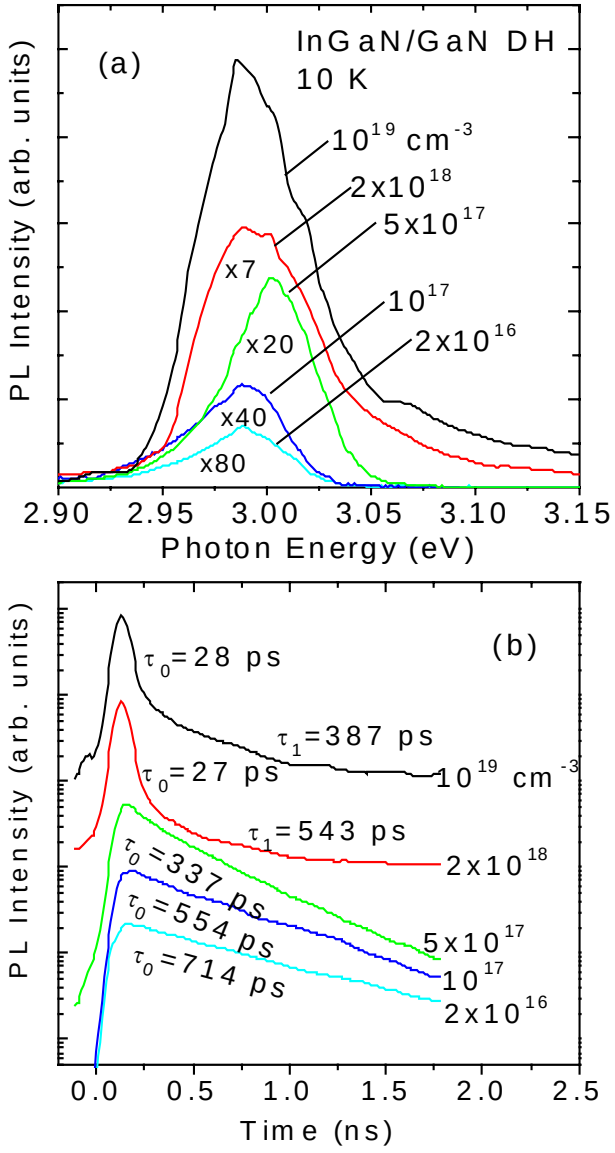

Figure 5.4. (a) Time integrated PL spectra and (b) time resolved PL intensities at different carrier densities of the InGaN sample.

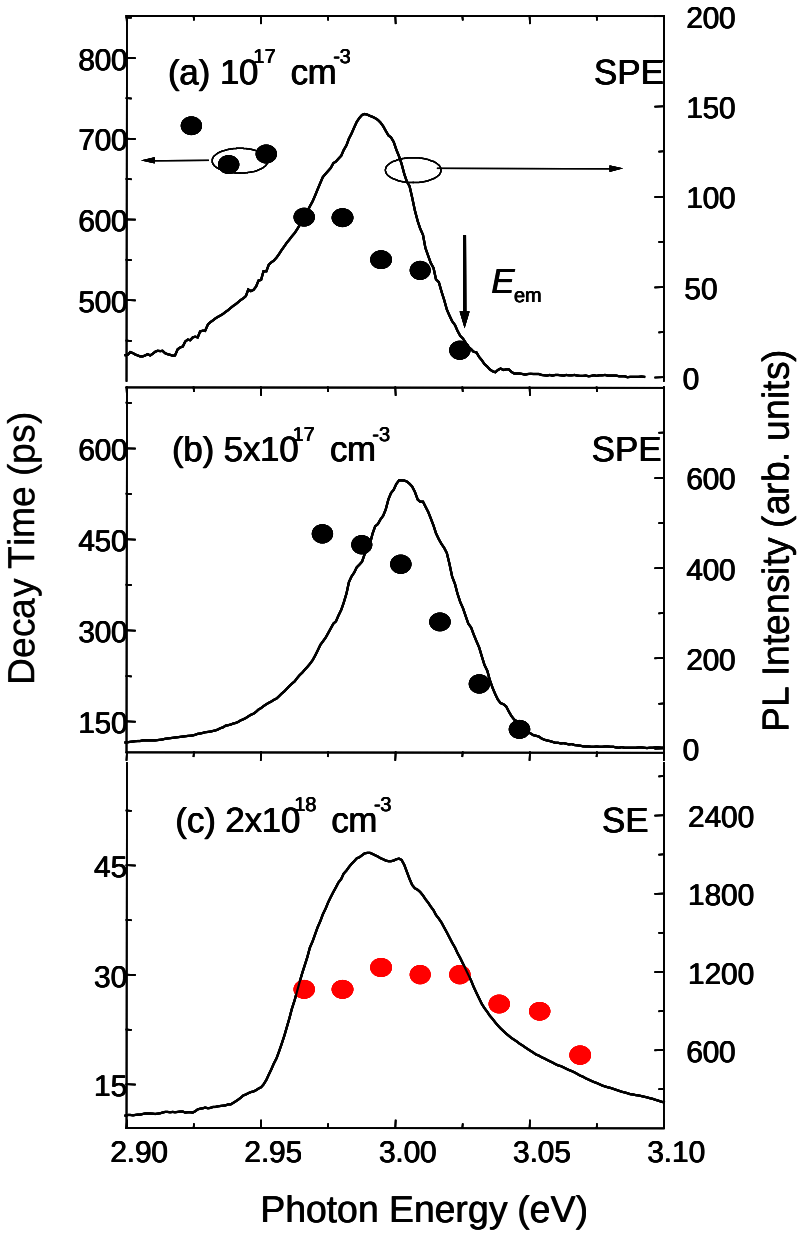

Figure 5.5. The time integrated PL spectra of the InGaN sample at three different carrier densities. The dots are effective recombination lifetime at the specific photon energy.

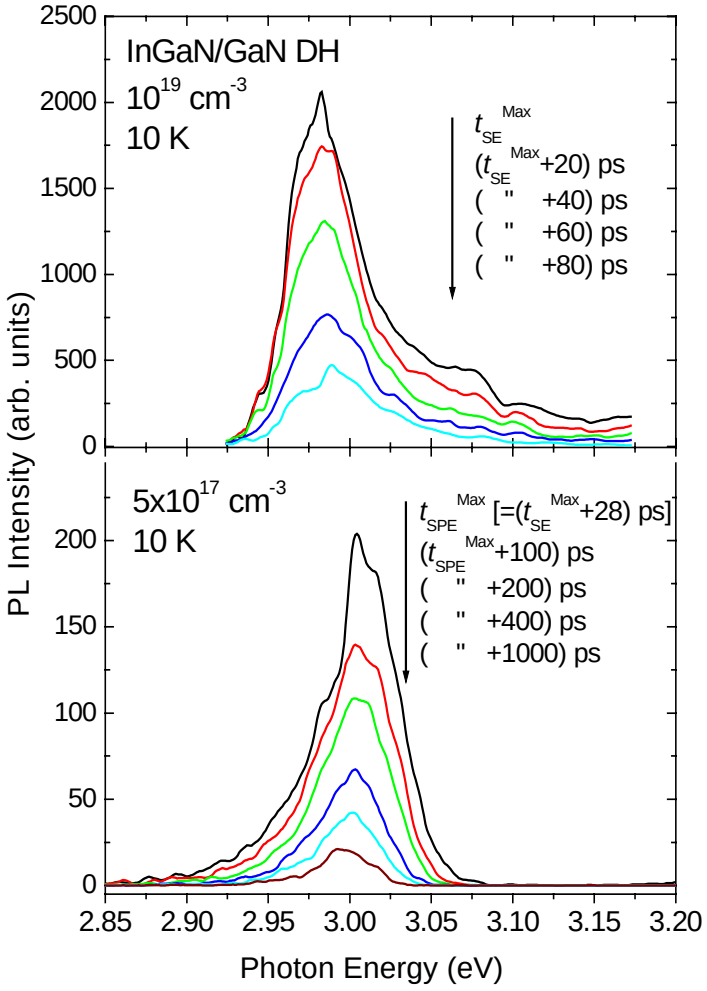

Figure 5.6. Temporal evolution (a) stimulated and (b) spontaneous emission of the InGaN sample for carrier densities of 10^{19} cm^{-3} and 5×10^{17} cm^{-3} respectively.

CHAPTER VI

Summary

The group-III nitrides have found viable applications and renew interest in recent years. This thesis tries to explore some of the emission properties in various nitride structures.

Gain mechanisms in $Al_{0.17}Ga_{0.83}N$ alloys over the temperature range from 30 K to room temperature were studied by examining relative shifts between the spontaneous and stimulated emission peaks as well as by evaluating the carrier densities required to generate gain in this material system. Conclusion was made that the dominant gain mechanism over the entire temperature range studied for the $Al_{0.17}Ga_{0.83}N$ sample is recombination of an electron hole plasma. The observed optical properties of AlGaN make it a leading candidate for the development of UV laser diodes.

The optical properties of a GaN epilayer and a GaN/AlGaN double heterostructure grown by HVPE were studied and compared to those of to a high quality MOCVD-grown GaN epilayer. Stimulated emission was obtained for both the HVPE-grown GaN epilayer and the GaN/AlGaN double heterostructure at 10 K and room temperature. It was found that the stimulated emission threshold and photoluminescence efficiency of the HVPE-grown samples are similar to those of high-quality MOCVD-grown structures. The results show that HVPE-grown nitrides have potential for UV – visible photonics device applications.

$In_xGa_{1-x}N$ with x values of 0.4, 1.5, and 2.4 % were studied. The S-shaped temperature dependence of PL peak energies gives evidence to indium segregation (typical of InGaN) in the samples, which causes composition fluctuation and carrier

localization leading to higher spontaneous emission intensity at RT. Stimulated emission at both 10 K and room temperature was observed for all three samples. Dramatic decrease of SE threshold is observed as indium content increase to 1.5%.

Hot carrier dynamics in an InGaN thin film was studied using femtosecond pump probe and time resolved photoluminescence spectroscopy at 10 K. Two successive LO phonon emission was clearly observed. As hot carriers relax, optical gain was observed, resulting in stimulated emission, with a threshold carrier density of 1×10^{18} cm^{-3}. SE was attributed to recombination of an electron hole plasma from band to band transitions.

Further improvement of performance of the GaN based opto-electronic devices requires exploration of new structures and new growth methods. New fabrication methods are required and are being done vigorously in both the industries and in the academia.

References:

1. S. Nakamura, M. Senoh, S. Nagahama, N. Iwasa, T. Yamada, T. Matsushita, H. Kiyoku, and Y. Sugimoto, Jpn. J. Appl. Phys. **35**, L74 (1996).

2. S. C. Jain, M. Willander, J. Narayan, and R. Van Overstraeten, J. Appl. Phys. **87**, 965 (2000).

3. J. J. Song and Wei Shan, *Group III Nitride Semiconductor Compounds: Physics and Applications,* Oxford Univ. Press, New York, 1998.

4. R. Juza and H. Hahn, Z. Anorg. Allg. Chem. **234**, 282 (1938), **244**, 133 (1940).

5. H. P. Maruska and J. J. Tietjen, Appl. Phys. Lett. **15**, 327 (1969).

6. H. Amano, M. Kito, K.Hiramatsu, and I. Akasaki, Jpn. J. Appl. Phys. **28**, L2112(1989).

7. F. A. Ponce, *Group III Nitride Semiconductor Compounds: Physics and Applications*, edited by B. Gil, (Clarendon Press, Oxford, 1998).

8. O. Madelung, editor, *Semiconductor – Basic Data*, 2nd edition, (Springer-Verlag, Berlin, 1996).

9. X. A. Cao and S. D. Arthur, Appl. Phys. Lett. **85**, 3971 (2004).

10. J. J. Song and W. Shan, *Group III Nitride Semiconductor Compounds: Physics and applications*, edited by B. Gil, (Clarendon Press, Oxford, 1998), pp. 182-241.

11. See, for example, J. J. Song and W. Shan, in *Properties, Processing and Applications of Gallium Nitride and Related Semiconductors*, edited by J. H. Edgar, S. Strite, I. Akasaki, H. Amano, and C. Wetzel. (Michael Faraday House, London, 1999), 596.
12. S. Bidnyk, B. D. Little, J. J. Song, and T. Schmidt, Appl. Phys. Lett. **75**, 2163 (1999).
13. S. Bidnyk, J. B. Lam, B. D. Little, Y. H. Kwon, J. J. Song, G. E. Bulman, H. S. Kong, and T. J. Schmidt, Appl. Phys. Lett. **75**, 3905 (1999).
14. L. Eckey, J. Holst, V. Kutzer, A. Hoffmann, I. Broser, O. Ambacher, M. Stutzmann, H. Amano, and I. Akasaki, Mat. Res. Soc. Symp. Proc. **468**, 237 (1997).
15. T. J. Schmidt, Y. H. Cho, J. J. Song, and W. Yang, Appl. Phys. Lett. **74**, 245 (1999).
16. S. Bidnyk, T. J. Schmidt, B. D. Little, and J. J. Song, Appl. Phys. Lett. **74**, 1 (1999).
17. S. Bidnyk, Ph. D. Thesis, Oklahoma State University, pp. 69-70 (1999).
18. A. J. Fischer, W. Shan, J. J. Song, Y. C. Chang, R. Horning, and B. Goldenberg, Appl. Phys. Lett. **71**, 1981 (1997).
19. T. J. Schmidt, Y. H. Cho, G. H. Gainer, J. J. Song, S. Keller, U. K. Mishra, and S. P. DenBaars, Appl. Phys. Lett. **73**, 1892 (1998).
20. Y. P. Varshni, Physica (Amsterdam) **34**, 149 (1967).
21. P. Riblet, H. Hirayama, A. Kinoshita, A. Hirata, and T. Sugano, Appl. Phys. Lett. **75**, 2241 (1999).
22. H. S. Kim, R. H. Mair, J. Li, J. Y. Lin, and H. X. Jiang, Appl. Phys. Lett. **76**, 1252 (2000).
23. R. Levy and J. B. Grun, Phys. Status Solidi A **22**, 11 (1974).
24. J. J. Song and W. Shan, *Group III Nitride Semiconductors Compounds: Physics and Applications*, edited by B. Gil (Clarendon, Oxford, 1998), pp. 186-191.

25. Y. H. Cho, G. H. Gainer, A. J. Fischer, J. J. Song, S. Keller, U. K. Mishra, and S. P. DenBaars, Appl. Phys. Lett. **73**, 1370 (1998).
26. S. Bidnyk, T. J. Schmidt, Y. H. Cho, G. H. Gainer, J. J. Song, S. Keller, U. K. Mishra, and S. P. DenBaars, Appl. Phys. Lett. **72**, 1623 (1998).
27. Nichia website, "www.nichia.com."
28. S. Bidnyk, J. B. Lam, B. D. Little, Y. H. Kwon, and J. J. Song, Appl. Phys. Lett. **75**, 3905 (1999).
29. I. Akasaki, S. Sota, H. Sakai, T. Tanaka, M. Koike, and H. Amano, Electron. Lett. **32**, 1105 (1996).
30. A. Usui, H. Sunakawa, A. Sakai, and A. A. Yamaguchi, Jpn. J. Appl. Phys. Part 2, **36**, L899 (1997).
31. B. J. Skromme, J. Jayapalan, R. P. Vaudo, and V. M. Phanse, Appl. Phys. Lett. **74**, 2358 (1999).
32. M. K. Kelly, R. P. Vaudo, V. M. Phanse, L. Gorgens, O. Ambacher and M. Stutzmann, Jpn. J. Appl. Phys. Part 2, **38**, L217 (1999).
33. S. Nakamura, M. Senoh, S. I. Nagahama, N. Iwasa, T. Yamada, T. Matsushita, H. Kiyoku, Y. Sugimoto, T. Kozaki, H. Umemoto, M. Sano, and K. Chocho, Appl. Phys. Lett. **73**, 832 (1998).
34. M. Kuramoto, C. Sasaoka, Y. Hisanaga, A. Kimura, A. A. Yamaguchi, H. Sunakawa, N. Kuroda, M. Nido, A. Usui, and M. Mizuta, Japn. J. Appl. Phys. **38**, L184 (1999).
35. W. Shan, T. J. Schmidt, R. J. Hauenstein, and J. J. Song, Appl. Phys. Lett. **66**, 3492 (1995).

36. S. Hearne, E. Chason, J. Han, J. A. Floro, J. Figiel, J. Hunter, H. Amano, I. S. T. Tsong, Appl. Phys. Lett. **74**, 356 (1999).

37. S. Bidnyk, T. J. Schmidt, B. D. Little and J. J. Song, Appl. Phys. Lett. **74**, 1 (1999).

38. W. Gotz, L. T. Romano, J. Walker, N. M. Johnson, and R. J. Molnar, Appl. Phys. Lett. **72**, 1214 (1998).

39.T. Tawara, H. Gotoh, T. Akasaka, N. Kobayashi, and T. Saitoh, Appl. Phys. Lett. **83**, 830 (2003).

40. K. S. Ramaiah, Y. K. Su, S. J. Chang, C. H. Chen, F. S. Juang, H. P. Liu, and I. G. Chen, Appl. Phys. Lett. **85**, 401 (2004).

41. S. Nakamura and G. Fasol, *The Blue Laser Diode* (Springer, Berlin 1997).

42. Y.-H. Kwon, G. H. Gainer, S. Bidnyk, Y. H. Cho, J. J. Song, M. Hansen, and S. P. DenBaars, Appl. Phys. Lett. **75**, 2545 (1999).

43. Yong-Hoon Cho, G. H. Gainer, A. J. Fischer, J. J. Song, S. Kelly, U. K. Mishra, and S. P. DenBaars, Appl. Phys. Lett. **73**, 1370 (1998).

44. S. F. Chichibu, M. Sugiyama, T. Onuma, T. Kitamura, H. Nakanishi, T. Kuroda, A. Tackeuchi, T. Sota, Y. Ishida, H. Okumura, Appl. Phys. Lett. **79**, 4319 (2001).

45. C. H. Chen, H. J. Chang, Y. F. Chen, W. S. Fann, H. X. Jiang and J. Y. Lin, Appl. Phys. Lett. **79**, 3806 (2001).

46. S. Nakamura, MRS Internet J. Nitride Semicond. Res. **2**, 5 (1997).

47. Y. C. Chang and H. Yao, Phys. Rev. B **54**, 11 517 (1996).

48. J. Shah, *Ultrafast Spectroscopy of Semicimductors and Semiconductor Nanostructures* (Springer-Verlag, Berlin, 1996), p. 23.

49. The carrier density was calculated using the band filling factor [1-f_e-f_h] (see p. 22 in Ref. 3), assuming a simple parabolic band structure and f_e=f_h. The nominal excitation energy densities were measured in PP and TRPL experiments. A calibration factor was obtained by comparison between band filling density and nominal density. Carrier density in TRPL measurements were determined with the calibration factor.
50. S. Chichibu, T. Azuhata, T. Soda, and S. Nakamura, Appl. Phys. Lett. **69**, 4188 (1996).
51. Y. Narukawa, Y. Kawahami, Sz. Fujita, and S. Nakamura, Phys. Rev. B **55**, 1938 (1997).
52. M. Smith, G. D Chen, J. Y. Lin, H. X. Jiang, M. A. Khan, and Q. Chen, Appl. Phys. Lett. **69**, 2837 (1996).
53. Y. –H. Cho, T. J. Schmidt, S. Bidnyk, G. H. Gainer, J. J. Song, S. keller, U. K. Mishra, and S. P. DenBaars, Phys. Rev B. **61**, 7571 (2000).
54. J. L. Oudar, D. Hulin, A. Migus, A. Antonetti, and F. Alexandre, Phys. Rev. Lett. **55**, 2074 (1985).
55. K. T. Tsen, D, K. Ferry, A. Botchkarev, B. Sverdlov, A. Salvador, and H. Morkoç, Appl. Phys. Lett. **72**, 2132 (1998).
56. V. Yu. Davudov, V. V. Emtsev, I. N. Goncharuk, A. N. Smironv, V. D. Petrikov, V. V. Mamutin, V. A. Vekshin, S. V. Ivanov, M. B. Smironv, and T. Inushirma, Appl. Phys. Lett. **75**, 3297 (1999).
57. T. Elsaesser, J. Shah, L. Rota, and P. Lugli, Phys. Rev. Lett. **66**, 1757 (1991).
58. J. Shah, A. Pinczuk, A. C. Gossard, and W. Wiegmann, Phys. Rev. Lett. **54**, 2045 (1985).

59. C. K. Sun, F. Vallée, S. Keller, J. E. Bowers, and S. P. DenBaars, Appl. Phys. Lett. **70**, 2004 (1997).

60. T. Gong, P. M. Fauchet, J. F. Young, and P. J. Kelly, Phys. Rev. b **44**, 6542 (1991).

61. C. V. Shank, R. L. Fork, R. Yen, J. Shah, B. I. Greene, A. C. Gossard, and C. Weisbuch, Solid State Commun. **47**. 981 (1983).

62. Y. Kawakami, Y. Narukawa, K. Omae, S. Fujita, and S. Nakamura, Appl. Phys. Lett. **77**, 2151 (2000).

63. E. Cohen and M. D. Sturge, Phys. Rev. B **25**, 3828 (1982); S. Permogorov and A. Reznitsky, J. Lumin. **52**, 201 (1992).

64. A. Satake, Y. Masumoto, T. Miyajima, T. Asatsuma, F. Nakamura, and M. Ikeda, Phys. Rev. b **57**, 2041 (1998).

65. N. F. Mott and E. A. Davis, Electronic processes in NonCrystalline Materials, 2nd ed. (Oxford University, England, 1979).

66. W. Fang and S. L. Chuang, Appl. Phys. Lett. **67**, 751 (1995).

67. Y. –K. Song, M. Kuball, A. V. Nurmikko, G. E. Bulman, K. Doverspike, S. T. Sheppard, T. W. Weeks, and M. Leonard, Appl. Phys. Lett. **72**, 1418 (1998).

68. T. Takeuchi, S. Sota, M. Katsuragawa, M. Komori, H. Takeuchi, H. Amano, and I. Akasaki, Jpn. J. Appl. Phys., Part 2 **36**, L382 (1997).

69. C. Gourdon and P. Lavallard, Phys. Status Solidi B **153**, 641 (1989).

70. M. Oueslati, C. Benoit à la Guillaume, and M. Zouaghi, Phys. Rev. B **37**, 3037 (1988).

71. J. A. Kash, A. Ron, andE. Cohen, Phys. Rev. B **28**, 6147 (1983).

APPENDIX

Publications and presentations

The following are refereed publications and conference presentations generated in research works leading to this thesis.

Publications:

"Polarization dependence of the excitonic optical Stark effect in GaN," C. K. Choi, J. B. Lam, G. H. Gainer, S. K. Shee, J. S. Krasinski, J. J. Song, and Yia-Chung Chang, Phys. Rev. B **65**, 155206 (2002).

"The excitonic optical Stark effect in GaN," C. K. Choi, Yia-Chung Chang, J. B. Lam, G. H. Gainer, S. K. Shee, J. S. Krasinski, and J. J. Song, Phys. Stat. Sol. (a) **190**, 99 (2002).

"Effect of the number of wells on optical and structural properties in InGaN quantum well structures grown by MOCVD," H.-K. Yuh, E. Yoon, S. K. Shee, J. B. Lam, C. K. Choi, G. H. Gainer, G. H. Park, S. J. Hwang, and J. J. Song, J. Appl. Phys. **91**, 3483 (2002).

"Femtosecond pump-probe spectroscopy and time-resolved photoluminescence of an InGaN/GaN double heterostructure," C. K. Choi, B. D. Little, Y. H. Kwon, J. B. Lam, J. J. Song, Y. C. Chang, S. Keller, U. K. Mishra, and S. P. DenBaars, Phys. Rev. B **63,** 195302 (2001).

"Well thickness dependence of emission from GaN/AlGaN separate confinement heterostructures," G. H. Gainer, Y. H. Kwon, J. B. Lam, S. Bidnyk, A. Kalashyan, J. J. Song, S. C. Choi and G. M. Yang, Appl. Phys. Lett. **78,** 3890 (2001).

"Optical properties and lasing in (In,Al)GaN-based structures," S. Bidnyk, G. H. Gainer, S. K. Shee, J. B. Lam, B. D. Little, T. Sugahara, J. Krasinski, Y. H. Kwon, G. H. Park, S. J. Hwang, J. J. Song, G. E. Bulman, and H. S. Kong, Phys. Stat. Sol. (a) **183**, 105 (2001).

"Growth of submicron AlGaN/GaN/AlGaN heterostructures by hydride vapor phase epitaxy (MVPE)," D. Tsvetkov, Yu. Melnik, A. Davydov, A. Shapiro, O. Kovalenkov, J. B. Lam, J. J. Song, and A. Dmitiev, Phys. Stat. Sol. (a) **188**, 428 (2001).

"Effect of well thickness on GaN/AlGaN separate confinement heterostructure emission," G. Gainer, Y. Kwon, J. Lam, S. Bidnyk, A. Kalashyan, J. Song, S. Choi, and G. Yang, Phys. Stat. Sol. (a) **188**, 857 (2001).

"Comparative study of HVPE- and MOCVD-grown nitride structures for UV lasing application," J. B. Lam, G. H. Gainer, S. Bidnyk, Amal Elgawadi, G. H. Park, J.

Krasinski, J. J. Song, D. V. Tsvetkov, and V. A. Dmitriev, Mat. Res. Soc. Symp. **639**, G6.4 (2001).

"MOCVD growth, stimulated emission and time resolved PL studies of InGaN/(In)GaN MQWs: well and barrier thickness dependence," S. K. Shee, Y. H. Kwon, J. B. Lam, G. H. Gainer, G. H. Park, S. J. Hwang, B. D. Little, and J. J. Song, J. Cryst. Growth **221**, 373 (2000).

"Optical properties of (Al)GaN-based structures for near- and deep-ultraviolet emitters," S. Bidnyk, J. B. Lam, Y. H. Kwon, G. H. Gainer, B. D. Little, and J. J. Song, Proc. Int. Workshop on Nitride Semiconductors (IWN2000), IPAP Conf. Series 1, 567 (2000).

"Dynamics of anomalous optical transition in $Al_xGa_{1-x}N$ alloys," Y. H. Cho, G. H. Gainer, J. B. Lam, J. J. Song, Phys. Rev. B **61**, 7203 (2000).

"Study of gain mechanisms in AlGaN in the temperature range of 30-300 K," J. B. Lam, S. Bidnyk, G. H. Gainer, B. D. Little, J. J. Song, and W. Yang, Appl. Phys. Lett. **77**, 4101 (2000).

"Microcavity-based semiconductor lasers for near- and deep-UV applications," S. Bidnyk, J. B. Lam, B. D. Little, Y. H. Kwon, J. J. Song, G. E. Bulman, and H. S. Kong, Conference on Lasers and Electro-Optics (CLEO) 2000 Technical Digest, CMG5 (2000).

"A comparative study of AlGaN and GaN-based lasing structures for near- and deep-UV applications," S. Bidnyk, J. B. Lam, G. H. Gainer, B. D. Little, Y. H. Kwon, J. J. Song, G. E. Bulman, and H. S. Kong, Mat. Res. Soc. Symp. Proc. T3.8, 316 (2000).

"Dynamics of anomalous temperature-induced emission shift in MOCVD-grown (Al, In)GaN thin films," Y. H. Cho, G. H. Gainer, J. B. Lam, J. J. Song, W. Yang, and W. Jhe, Mat. Res. Soc. Symp. Proc. **595** and MRS Internet J. Nitride Semicond. Res. **5S1**, W11.57 (2000).

"Microstructure-based lasing in GaN/AlGaN separate confinement heterostructures," S. Bidnyk, J. B. Lam, B. D. Little, G. H. Gainer, Y. H. Kwon, J. J. Song, G. E. Bulman, and H. S. Kong, Mat. Res. Soc. Symp. Proc. **595**, W11.22 (1999); MRS Internet J. Nitride Semicond. Res. **5S1**, W11.22 (2000).

"Comparative study of near-threshold gain mechanisms in GaN epilayers and GaN/AlGaN separate confinement heterostructures," S. Bidnyk, J. B. Lam, B. D. Little, G. H. Gainer, Y. H. Kwon, J. J. Song, G. E. Bulman, and H. S. Kong, The International Society for Optical Engineering (SPIE) Conf. Proc. **3947**, 126 (2000).

"Mechanism of efficient ultraviolet lasing in GaN/AlGaN separate confinement heterostructures," S. Bidnyk, J. B. Lam, B. D. Little, Y. H. Kwon, J. J. Song, G. E. Bulman, H. S. Kong, and T. J. Schmidt, Appl. Phys. Lett. **75**, 3905 (1999).

"Carrier recombination dynamics of $Al_xGa_{1-x}N$ epilayers grown by MOCVD," Y. H. Cho, G. H. Gainer, J. B. Lam, J. J. Song, W. Yang, and S. A. McPherson, Mat. Res. Soc. Symp. Proc. **572**, 457 (1999).

"Comparative study of emission from highly excited (In, Al) GaN thin films and heterostructures," B. D. Little, S. Bidnyk, T. J. Schmidt, J. B. Lam, Y. H. Kwon, J. J. Song, S. Keller, U. K. Mishra, S. P. DenBaars, and W. Yang, Mat. Res. Soc. Symp. Proc. **572**, 351 (1999).

"A comparison of the optical characteristics of AlGaN, GaN, and InGaN thin films," Y. H. Cho, T. J. Schmidt, G. H. Gainer, J. B. Lam, J. J. Song, S. Keller, U. K. Mishra, S. P. DenBaars, W. Yang, D. S. Kim, and W. Jhe, phys. stat. sol. **216**, 227 (1999).

Presentations:

"Excitonic optical Stark effect in GaN," C. K. Choi, J. B. Lam, G. H. Gainer, S. K. Shee, J. S. Krasinski, J. J. Song, and Y. C. Chang, SPIE Photonics West, **4643-16**, San Jose, CA (January 20-25, 2002).

"Carrier dynamics in a highly excited $In_xGa_{1-x}N$/GaN double heterostructure," C. K. Choi, J. B. Lam, G. H. Park, S. J. Hwang, J. S. Krasinski, J. J. Song, Y. C. Chang, S. Keller, U. K. Mishra, and S. P. DenBaars, the Fourth International Conference on Nitride Semiconductors, Denver, CO (Jul 16 – 20, 2001).

"The excitonic ac Stark effect in a GaN epilayer," C. K. Choi, J. B. Lam, G. H. Gainer, S. K. Shee, J. J. Song, and Y. C. Chang, the Fourth International Conference on Nitride Semiconductors, Denver, CO (Jul 16 – 20, 2001).

"Effect of well thickness on GaN/AlGaN separate confinement heterostructure emission," G. H. Gainer, Y. H. Kwon, J. B. Lam, S. Bidnyk, A. Kalashyan, J. J. Song, S. C. Choi, and G. M. Yang, the Fourth International Conference on Nitride Semiconductors, Denver, CO (Jul 16 – 20, 2001).

"Temperature dependence of transmission and emission spectra in MOCVD-grown AlGaN ternary alloys," Y. H. Cho, G. H. Gainer, J. B. Lam, J. J. Song, and W. Yang, the Fourth International Conference on Nitride Semiconductors, Denver, CO (Jul 16 – 20, 2001).

"Optical and X-ray Studies of MOCVD-grown InGaN Epilayers with Low Indium Concentration," G. H. Park, J. B. Lam, S. J. Hwang, S. K. Shee, T. Sugahara, G. H. Gainer, Amal Elgawadi, and J. J. Song, American Physical Society March Meeting, Seattle, WA (March 12 -16, 2001).

"Comparative study of HVPE- and MOCVD- grown laser structures for UV applications," J. B. Lam, S. Bidnyk, A. Elgawadi, G. H. Park, J. Krasinski, J. J. Song, D. V. Tsvetkov, V. A. Dmitriev, Mat. Res. Soc. Fall 2000, Boston, MA (November 27 - December 1, 2000).

"Optical properties and lasing in (In,Al)GaN-based structures," J. J. Song, S. Bidnyk, J. B. Lam, G. H. Gainer, and Y. H. Kwon, ISPSA 2000 (invited), Cheju, Korea (November 1 –3, 2000).

"Absorption, emission, and carrier dynamics study of MOCVD-grown $Al_xGa_{1-x}N$ Alloys," Y. H. Cho, G. H. Gainer, J. B. Lam, J. J. Song, W. Yang, and T. W. Kang, ISPSA 2000, Cheju, Korea (November 1 –3, 2000).

"Optical properties and lasing in (In,Al)GaN-based structures," S. Bidnyk, J. B. Lam, Y. H. Kwon, G. H. Gainer, S. K. Shee, G. H. Park, S. J. Hwang, B. D. Little, and J. J. Song, International Workshop on Physics of Light-matter Coupling in Nitrides, France (October 8 – 12, 2000).

"Optical properties of (Al)GaN-based structures for near- and deep-ultraviolet emitters," S. Bidnyk, J. B. Lam, Y. H. Kwon, G. H. Gainer, B. D. Little, and J. J. Song, Int. Workshop on Nitride Semicond. (IWN2000), TA2-3, Nagoya, Japan (September 24 - 27, 2000).

"MOCVD growth, stimulated emission and time resolved PL studies of InGaN/(In)GaN MQWs: well and barrier thickness dependence," S. K. Shee, Y. H. Kwon, J. B. Lam, G. H. Gainer, G. H. Park, S. J. Hwang, B. D. Little, J. J. Song, The Tenth International Conference on Metalorganic Vapor Phase Epitaxy (ICMOVPE-X), Sapporo, Japan (June 5 - June 9, 2000).

"Study of gain mechanisms in $Al_xGa_{1-x}N$ in the temperature range of 30 to 300 K," J. B. Lam, S. Bidnyk, G. H. Gainer, B. C. Little, J. J. Song, and W. Yang, Conference on Lasers and Electro-Optics (CLEO) 2000, CMG1, 76, San Francisco, CA (May 7 - 12, 2000).

"Microcavity-based semiconductor lasers for near- and deep-UV applications," S. Bidnyk, J. B. Lam, B. D. Little, Y. H. Kwon, J. J. Song, G. E. Bulman, and H. S. Kong, Conference on Lasers and Electro-Optics (CLEO) 2000, CMG5, 78, San Francisco, CA (May 7 - 12, 2000).

"GaN/AlGaN SCH UV semiconductor lasers: Effect of GaN well thickness on lasing efficiency," G. H. Gainer, Y. H. Kwon, J. B. Lam, A. Kalashyan, J. J. Song, S. C. Choi and G. M. Yang, Conference on Lasers and Electro-Optics (CLEO) 2000, CMG4, San Francisco, CA (May 7 - 12, 2000).

"A comparative study of AlGaN- and GaN-based lasing structures for near- and deep-UV applications," S. Bidnyk, J. B. Lam, B. D. Little, Y. H. Kwon, and J. J. Song, Mat. Res. Soc. Spring Meeting 2000, T3.8, 316, San Francisco, CA (April 24 - 28, 2000).

"Comparative study of gain mechanisms in GaN epilayers and GaN/AlGaN separate confinement heterostructures," S. Bidnyk, J. B. Lam, B. D. Little, G. Gainer, J. J. Song, American Physical Society March Meeting, R17.10, 739, Minneapolis, MN (March 20-24, 2000).

"Study of stimulated emission in AlGaN thin films in the temperature range of 30 K to 300 K," J. B. Lam, S. Bidnyk, G. Gainer, B. Little, J. J. Song, and W. Yang, American Physical Society March Meeting, R17.11, 740, Minneapolis, MN (March 20-24, 2000).

"Recent progress in the development of (Al, Ga)N lasing structures for near- and deep-ultraviolet emitters," S. Bidnyk, J. B. Lam, B. D. Little, and J. J. Song, Sixth Wide Bandgap III-Nitride Workshop, MP-1.4, Richmond, VA (March 12-15, 2000).

"Comparative study of near-threshold gain mechanisms in GaN epilayers and GaN/AlGaN separate confinement heterostructures," S. Bidnyk, J. B. Lam, B. D. Little, G. H. Gainer, Y. H. Kwon, and J. J. Song, The International Society for Optical Engineering (SPIE) Photonics West 2000, 3947-24, 126, San Jose, CA (January 23-28, 2000).

"Dynamics of anomalous temperature-induced emission shift in MOCVD-grown (Al, In)GaN thin films," Yong-Hoon Cho, G. H. Gainer, J. B. Lam, J. J. Song, W, Yang, and W. Jhe, Mat. Res. Soc. Fall 99, Boston, MA (November 29 - December 3, 1999).

"Mechanism of efficient ultraviolet lasing in a GaN/AlGaN separate confinement heterostructure," S. Bidnyk, J. B. Lam, B. D. Little, G. H. Gainer, Y. H. Kwon, J. J. Song, G. E. Bulman, and H. S. Kong, Mat. Res. Soc. Fall 99, Boston, MA (November 29 - December 3, 1999).

"A comparison of the optical characteristics of AlGaN, GaN, and InGaN thin films," Y. H. Cho, T. J. Schmidt, G. H. Gainer, J. B. Lam, J. J. Song, S. Keller, U. K. Mishra, S. P. DenBaars, W. Yang, D. S. Kim, and W. Jhe, The Third International Conference on Nitride Semiconductors (ICNS3), Montpellier, France (July 5-9, 1999).

"Optical nonlinearities in the band edge region of highly excited (Al, In)GaN thin films studied via femtosecond and nanosecond optical pump-probe spectroscopy," T. J. Schmidt, A. J. Fischer, J. B. Lam, and J. J. Song, The Third International Conference on Nitride Semiconductors (ICNS3), Montpellier, France (July 5-9, 1999).

"Carrier recombination dynamics of $Al_xGa_{1-x}N$ epilayers grown by MOCVD," Y. H. Cho, G. H. Gainer, J. B. Lam, J. J. Song, W. Yang, and S. A. McPherson, Mat. Res. Soc. Spring Meeting, San Francisco, CA (April 5-9, 1999).

"Comparative study of emission from highly excited (In, Al) GaN thin films and heterostructures," B. D. Little, S. Bidnyk, T. J. Schmidt, J. B. Lam, Y. H. Kwon, J. J. Song, S. Keller, U. K. Mishra, S. P. DenBaars, and W. Yang, Mat. Res. Soc. Spring Meeting, Y7.4, 388, San Francisco, CA (April 5-9, 1999).

VITA

Jack Biu Lam

Candidate for the Degree of

Doctor of Philosophy

Thesis: OPTICAL STUDIES OF GAN-BASED LIGHT EMITTING STRUCTURES

Major Field: Photonics

Biographical:

Personal Data: Born in Haikou, Hainan Island, China, on January 17, 1976, the son of Hung Cheung Lam and Mei Ling Ng.

Education: Graduated from Stuyvesant High School, New York, NY in1994; received Honor Diploma in Physics from State University of New York at Stony Brook, Stony Brook, NY in1998. Completed the requirements for the Doctor of Philosophy Degree with a major in Photonics at Oklahoma State University in May 2005.

Professional Experience: Employed by Oklahoma State University, Center for Laser and Photonics Research and Department of Physics as a graduate research assistant, 1998 to 2001. Employed by Oklahoma State University, School of Electrical and Computer Engineering as teaching assistant, 2001 to 2004.

Professional Memberships: American Physical Society, Materials Research Society.

Name: Jack Biu Lam Date of Degree: May, 2005

Institution: Oklahoma State University Location: Stillwater, Oklahoma

Title of Study: OPTICAL STUDIES OF GAN-BASED LIGHT EMITTING STRUCTURES

Pages in Study: 62 Candidate for the Degree of Doctor of Philosophy

Major Field: Photonics

Scope and Method of Study: The optical properties of group-III Nitrides were systematically studied over a temperature range of 10 to 300 K. A large variety of light sources including femtosecond, picosecond, and nanosecond laser systems as well as continuous wave light sources were used to optically excite the samples in this study. The sample emission was detected with photomultiplier tubes, CCD cameras, and a streak camera. Particular emphasis was put on high-excitation density phenomena and the stimulated emission properties in the samples. Issues related to gain mechanisms, carrier localization, and hot carrier dynamics were addressed.

Findings and Conclusions: Gain mechanisms in AlGaN epilayer were examined, and conclusion was made that over the entire temperature range of 10 to 300 K, recombination of an electron hole plasma is responsible for optical gain. HVPE-grown GaN epilayer and GaN/AlGaN double heterostructure were shown to have good photoluminescence efficiency and stimulated emission properties similar to that of a high quality MOCVD-grown sample, making them excellent candidate for UV – visible light emitting applications. Incorporation of a small amount of In into GaN layers resulted in the familiar carrier localization that are well known to have existed in InGaN structures, and lead to efficient photo emission process. In femtosecond pump-probe and time-resolved photoluminescence spectroscopy of an InGaN sample, emission of two successive LO phonon was clearly observed. As hot carriers relax toward the band edge, optical gain was observed, resulting in stimulated emission of the sample. Stimulated emission was attributed to recombination of an electron hold plasma from band to band transition.

ADVISER'S APPROVAL: Jerzy Krasinski